Matthias J. Kogler, BSc

Influence of Absorber Layer Thickness, Composition and Organic Additives on the Performance of Polymer/Copper Indium Sulfide Hybrid Solar Cells

MASTER THESIS

to achieve the university degree of

Diplom-Ingenieur

Master's degree programme: Technical Chemistry

Submitted to

Graz University of Technology

Supervisor:

Assoc.Prof. Dipl.-Ing. Dr.techn. Gregor Trimmel

Institute for Chemistry and Technology of Materials

August 2016

AFFIDAVIT

I declare that I have authored this thesis independently, that I have not used other than the declared sources/resources, and that I have explicitly indicated all material which has been quoted either literally or by content from the sources used. The text document uploaded to TUGRAZonline is identical to the present master's thesis.

Graz, August 2016

Matthias J. Kogler

INFLUENCE OF ABSORBER LAYER THICKNESS, COMPOSITION AND ORGANIC ADDITIVES ON THE PERFORMANCE OF POLYMER/COPPER INDIUM SULFIDE HYBRID SOLAR CELLS

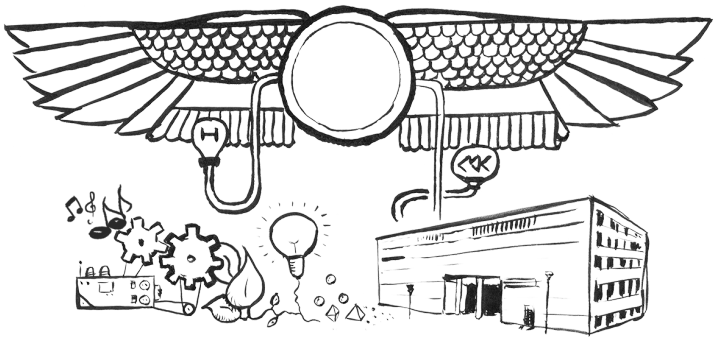

MATTHIAS J. KOGLER

„Komm setz dich neben mich, *Bumbi*.“

Bum•bala; Bum•bal od. Bum•bi [bumba'lla; bumba'll od. bu'mbi] NOMEN für **1.** Kind od. **2.** Tierjunges od. **3.** für ziemlich jedes kleine Ding: *steir.: Schau, a bumbala*. **4.** TIEFGRÜNDIGERE BEDEUTUNG zum Ausdruck von großväterlichen Liebe und Stolz für eine Person.

— Aus dem sehr originellen Vokabular des
Engelbert Gepp,
mein geliebter Großvater,
dem diese Arbeit gewidmet ist.

Bum•bala; Bum•bal or Bum•bi [bumba'lla; bumba'll or bu'mbi] NOUN for **1.** child or **2.** animal offspring or **3.** mostly any small thing: *steir.: Schau, a bumbala*. **4.** SUBLIMINAL MEANING to kindly express fatherly affenction to sb including to take pride in this person.

— From the very special vocabulary of
Engelbert Gepp,
my beloved Grandfather
to whom this work is dedicated to.

«Denn die Sonne scheint, ich ärgere mich über gar nichts,
was will ich mehr!»
— Janosch. Aus der Geschichte «Komm nach Iglau, Krokodil»

ACKNOWLEDGMENTS

I want to express my gratitude towards Assoc.Prof. Dipl.-Ing. Dr.techn. Gregor Trimmel, who gave me trough this thesis the opportunity to complete one big step in my academic career. Further, he established an atmosphere where I could work flexibly and with high self initiative. At the same time I knew I could always seek advice. Besides that, I enjoyed the positive attitude and, of course, working on the very interesting and important topic of this thesis itself. *Thank you very much.*

Outstanding, as well as, incredibly helpful was the expertise of Dipl.-Ing. Dr.techn. Thomas Rath. The certainty of having him as a counselor and the possibility of discussing ideas together improved my work significantly. *Thank you, Thomas.*

The support of a team is good. Being supported by an excellent team is even better. Thanks to Christina Buchmaier, Indira Zahirovic, Sebastian Höfler, as well as to Denise Bacher, Franz Pirolt, Manuel Hollauf, Raffael Rathner and Sebastian Dunst. You all contributed to the very comfortable and friendly working environment. *Thank you, guys.*

Further, Dipl.-Ing. Dr.techn. Astrid Knall was responsible for the synthesis of the conjugated polymer PPDTBT used in this work. Dipl.-Ing. Katrin Niegelhell performed the microscopy for the AFM images in this work. *Thank you, Astrid. Thank you, Katrin.*

Additionally, I want to thank two colleagues for their constant help in the last seven years by providing advice and urging me to make progress in my studies. The resulting friendship is an inestimable enrichment to me. *Thank you, Sina. Thank you, Anna.*

MEINER FAMILIE UND MEINEN FREUNDEN *möchte ich hiermit ganz speziellen Dank ausdrücken, für all die Unterstützung, die weit über meine akademische Laufbahn hinaus ging und wofür diese wenigen Zeilen nicht ausreichen. Besonderen Dank gilt meiner Mutter Karin dafür, mich zu dem Mann gemacht zu haben, der ich bin, und der (mit aller Bescheidenheit) doch ganz anständig geworden ist. Meinem Vater Walter dafür, mich stets so akzeptiert zu haben, wie ich bin, und der mich so mit Selbstbewusstsein gerüstet hat. Meinen Großeltern Margaretha und Engelbert für die beste großelterliche Unterstützung, die ich mir wünschen konnte, gemeinsam mit meinem Onkel Herbert. Meinen engen Freunden Marc und Jakob für die hervorragende Unterstützung in wichtigen Dingen wie Freizeitgestaltung und Entspannung. Und schlussendlich danke ich meiner Schwester Marie-Sofie für viele schöne und lustige Momente, wie sie nur Geschwister haben können.* Ich danke Euch.

ABSTRACT

In this work different polymers and additives where investigated in connection with polymer/copper indium sulfide (CIS) nanoparticle hybrid solar cells. The nanoparticles are formed in-situ from metal xanthate precursors within the polymer matrix via heat treatment below 200 °C.

For the main part of this work the conjugated polymer poly [N-9′-heptadecanyl-2,7-carbazole-alt-5,5-(4,7-di-2-thienyl-2′,1′,3′-benzo thiadiazole)] (PCDTBT) was used as the organic phase in the absorber layer. The application of a low molecular weight polymer led to a power conversion efficiency of 2.24% and a high fill factor of 59%. Changing to a higher molecular weight PCDTBT did not enhance the performance of the solar cells. Moreover, it was found that the exposure to air for five minutes increased the open circuit voltage, the short circuit current density, and the fill factor for devices with aluminum electrodes. A solar cell with a power conversion efficiency of 2.36 and a fill factor of 58% was produced by applying this air treatment. Furthermore, silver as top-electrode material showed good short circuit current density (higher than 7 mA/cm^2) which was reproducible. Such a device also showed the highest power conversion efficiency of 2.45% in this work. Its short circuit current density was above 11 mA/cm^2. Benzene-1,3-dithiol, pyridine, and 1,8-diiodoctane were investigated regarding their influence on the polymer/nanoparticle interface. Only benzene-1,3-dithiol showed a positive influence on the device parameters after a treatment with this compound.

Solar cells with the conjugated polymer poly[(5,6-difluoro-2,1,3-benzothiadiazol-4,7-diyl)-alt-(3,3‴-di(2-octyldodecyl)-2,2′;5′,2″;5″,2‴-quaterthiophen-5,5‴-diyl)] (PffBT4T-2OD) as the organic phase did not reveal good diode characteristics most likely due to the challenging processing of this polymer and difficulties in the fabrication of absorber layers with smooth surfaces and appropriate thicknesses.

Hybrid solar cells with 70 vol% CIS and the conjugated polymer poly[4,8-bis(5-(2-ethylhexyl)thiophen-2-yl)benzo[1,2-b:4,5-b′]dithiophene-2,6-diyl-1,4-bis(5-bromothiophen-2-yl)-6-(2-decyltetradecyl)-5H-pyrrolo[3,4-d] pyridazine-5,7(6H)-dione-5,5″-diyl] (PPDTBT) showed power conversion efficiencies up to 1.77%.

ZUSAMMENFASSUNG

In dieser Arbeit wurden Polymere und Additive für Polymer/Kupferindiumsulfid (CIS) Nanopartikel-Hybridsolarzellen untersucht. Die CIS Nanopartikel wurden via in-situ Route hergestellt. Dabei wurden die Nanopartikel direkt in der Polymermatrix bei unter 200 °C aus Metallxanthaten hergestellt.

Ein großer Teil dieser Arbeit befasst sich mit Poly[N-9'-heptadecanyl-2,7-carbazole-alt-5,5-(4,7-di-2-thienyl-2',1',3'-benzothiadiazole)] (PCDTBT) als konjugiertes Polymer im Aktivmaterial. Wurde ein niedermolekulares Polymer verwendet konnten eine Energieumwandlungseffizienz (PCE) von 2,24% und ein hoher Füllfaktor von 59% erhalten werden. Der Wechsel zu einem höher molekularen Polymer brachte keine Verbesserungen. Weiters wurde bei Solarzellen mit Aluminiumelektroden, die für fünf Minuten Raumluft ausgesetzt wurden, eine Erhöhung aller Zellparameter festgestellt. So erreichte eine Solarzelle, mit 70 vol% CIS in der Absorberschicht, einer PCE von 2,36% und einen Füllfaktor von 58%. Silber in Verwendung als Elektrodenmaterial war gut reproduzierbar und hohe Kurzschlussstromdichten (über 7 mA/cm²) wurden regelmäßig gemessen. Eine solche Solarzelle wies die höchste PCE dieser Arbeit mit 2,45% auf und wurde durch die Kurzschlussstromdichte von über 11 mA/cm² erreicht. Die Moleküle Benzen-1,3-dithiol, Pyridin und 1,8-Diiodoktan wurden auf ihren Einfluss auf das Polymer/Nanopartikel-Interface der Solarzellen untersucht. Dabei zeigte nur Benzen-1,3-dithiol eine positive Wirkung auf die Zellparameter.

Solarzellen mit dem Polymer Poly[(5,6-difluoro-2,1,3-benzothiadiazol-4,7-diyl)-alt-(3,3'''-di(2-octyldodecyl)-2,2';5',2'';5'',2'''-quaterthiophen-5,5'''-diyl)] (PffBT4T-2OD) wiesen keine guten Diodencharakteristiken auf, da es Schwierigkeiten bereitete Absorberschichten mit glatten Oberflächen und ausreichender Dicke herzustellen.

Hybridsolarzellen mit dem neuen konjugierten Polymer Poly[4,8-bis(5-(2-ethylhexyl)thiophen-2-yl)benzo[1,2-b:4,5-b']dithiophene-2,6-diyl-1,4-bis(5-bromothiophen-2-yl)-6-(2-decyltetradecyl)-5H-pyrrolo[3,4-d]pyridazine-5,7(6H)-dione-5,5''-diyl] (PPDTBT) erreichten eine PCE bis zu 1,77%.

CONTENTS

Part I

INTRODUCTION AND THEORY

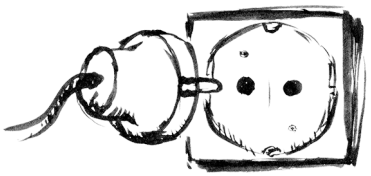

1

SOLAR ENERGY

1.1 A VAST ENERGY SUPPLY

The sun provides a vast amount of energy every day and for free. It is estimated that the energy of sunlight irradiated on earth in one hour can meet the global energy demand for a whole year [36]. Unfortunately, there is no cost-efficient technology yet, which allows the storage of this amount of electrical energy, but this example shows signs of a great opportunity.

At the same time world's energy demand is steadily rising, caused by population growth and industrial development. Regarding the amount of energy needed, the energy source does not only have to be economically viable, but also has to meet sustainability requirements. Challenges like energy storage or energy conversion during winter or cloudy periods of time have to be overcome, as well as the engineering part of improving materials. Resulting technologies should be safe, environmentally friendly and affordable.

Since the solar boom started in the 2000s, we are now at the point where photovoltaic (PV) technology is a realistic possibility to meet these modern requests. Over the last 10 years a decrease of over 80% in cost of PV electricity was observed [5] and new solar cell types have been developed which show attractive efficiencies comparable to silicon based cells.

Most advantages of PV technology are obvious and quite impressive. Once the system is established it will be sustainable, essentially emission and noise free. Additionally, solar technology can be implemented in small and truly mobile applications. Although, the share of the global electricity demand provided by solar energy increased tenfold from 2012 to 2014 (from 0.1 % to over 1% [36, 41]) and is further increasing, this share is still

very small. Currently, important tasks are to establish PV in our daily life, to make progress in advanced PV engineering as well as in education in this field. Ciriminna et al. [5] propose a *Solar Master* – a multidisciplinary graduate course – with the goal of raising awareness and understanding of solar energy as a critical future resource, and further developing and increasing public perception of solar energy systems.

1.2 SOLAR RADIATION

The sun is a very powerful energy source, but to use the sun's energy in order to generate electricity one must understand the solar radiation to harness its full potential.

Before the sunlight enters the atmosphere, the spectrum is almost identical to a black body spectrum at 5800 K. Then, gases in the atmosphere (O_3, O_2, CO_2, water vapor) absorb certain wavelengths. Because of this, the spectrum reaching earth's surface depends on the thickness of the atmospheric layer, through which the light has to cross. The system that has been established to classify this thickness assigns a certain air mass (AM) to global regions – a schematic depiction is shown in figure 1. At AM0 the light did not pass through the atmosphere – zero air mass means no absorption by atmospheric gases. At equatorial and tropical regions the light has passed the atmospheric layer one time. These regions are assigned to AM1. Most of the earth's population lives in tempered latitudes. Here AM1.5 applies as the light crosses an atmospheric layer 1.5 times thicker than for AM1, due to the angle of the light beam. These regions include e. g. Europe, the United States of America, China, and Japan. Compared to AM0, at AM1.5, some radiation intensity is lost due to absorptions from O_3 around 250 nm, from O_2 around 750 nm, from water around 950, 1150, 1400, 1900 and 2700 nm, and from CO_2 around 2025 and 2075 nm – see figure 2. Figure 2 also shows that solar radiation is strongest in the visible wavelengths range and in the near IR region. Therefore, solar cell materials

should efficiently absorb light in this region order to produce energy with high efficiency.

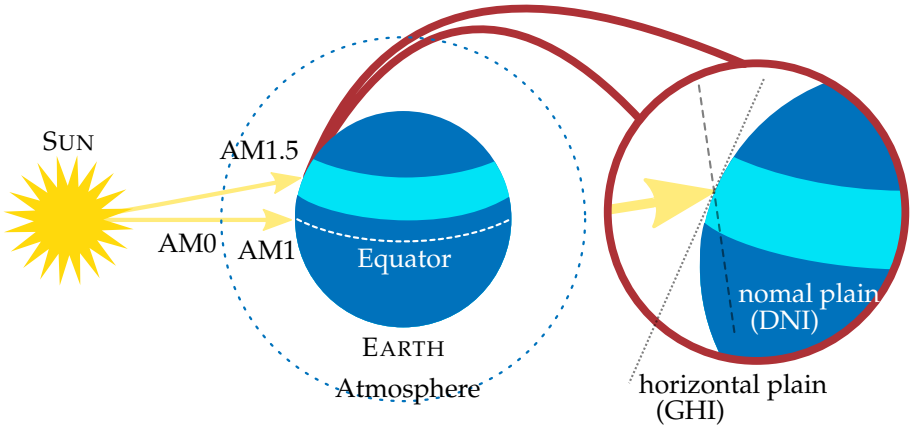

FIGURE 1: Scheme of the air masses and plains which influence the solar irradiation on earth. The light blue area shows earth's tempered latitudes.

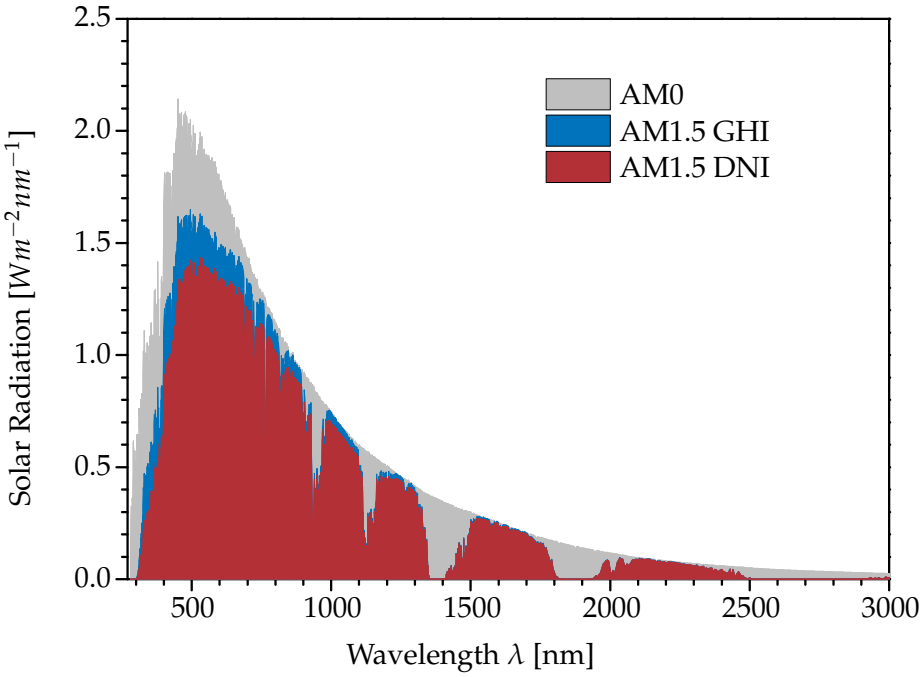

FIGURE 2: The standard solar spectra. Data taken from PV Education [31].

For solar cell module installations it is additionally important to consider how the panels are oriented regarding the direction of the incoming light. Consequently this also influences how regions on earth's surface can be evaluated concerning their suitability for such installations.

The global horizontal irradiation (GHI) is the irradiation of sunlight measured horizontally, whereas the direct normal irradiation (DNI) is

measured normal to the direction of the sunlight (both are shown in figure 2 for AM1.5). Usually an orientation of the panels directly towards the sunlight is beneficial for their power conversion efficiency (PCE). The worldmaps in figure 3 show the GHI (3a) and the DNI (3b) on earth's landmass with the corresponding energy in kWh/m², which could be utilized by PV technologies.

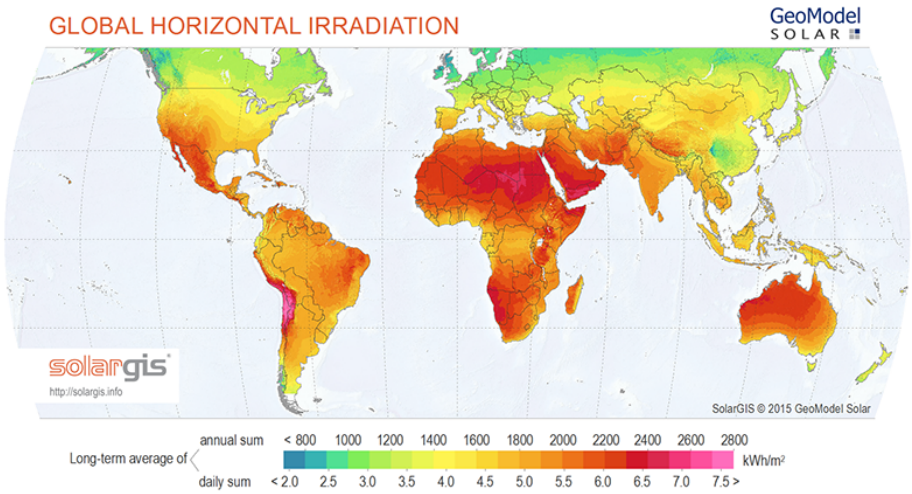

(A) GHI Solar Map © 2016 Solargis

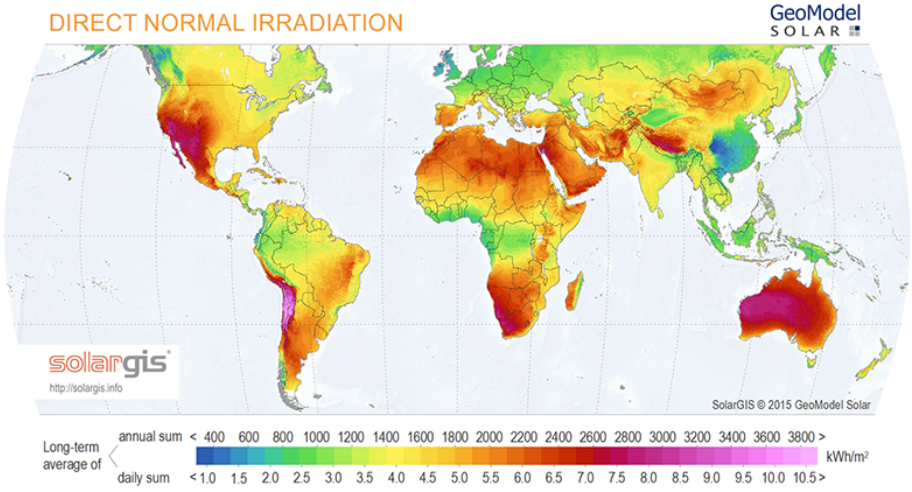

(B) DNI Solar Map © 2016 Solargis

FIGURE 3: Worldmaps showing GHI and DNI.

2

SOLAR CELLS

2.1 PHOTOVOLTAICS

The conversion of solar energy to electrical energy is based on the photoelectric effect – the charge-carrier generation by light in semiconductors. To use this effect for PV technologies a special material arrangement must be found which is able to carry out the following critical steps:

- An electron-hole-pair has to be generated from the energy of the absorbed light,
- the electron and the hole must be separated, and finally
- transported to the respective electrode to provide the electron and the hole to the outer circuit.

The term *hole* has become established to describe the vacancy which an excited electron leaves behind. The excited electron moves freely while other electrons can occupy the vacancy, leading to an apparently moving hole. In figure 4 a basic electron excitation scheme is depicted.

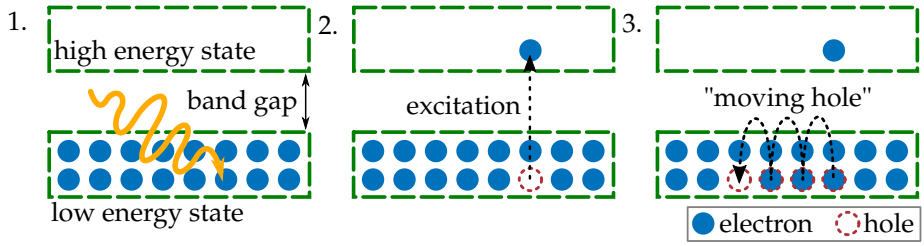

FIGURE 4: Electron-hole-pair generation and "moving" hole.

The absorption of light takes place in the active layer, resulting in an excitation of electrons. Two electrodes are applied onto the opposite sites

of the active layer, with or without applying further interfacial layers. Using different electrode materials is crucial in order to produce an internal electric field. The electric field is a result of the different work functions. This urges the electron and the hole to move in a predetermined direction.

To generate a freely moving electron (a separated electron-hole-pair) the electron must be excited by light into a high energy state. The electrons in a semiconductor can only be in a low or in a high energy state and – ignoring electronic defects such as traps – cannot attain a state in between. This defines a certain energetic distance and is called the *band gap*. The term band gap derives from classical inorganic semiconductors and describes the energetic distance of the valence and the conduction band. Concerning organic photovoltaics it is also used to describe the distance between the highest occupied molecular orbital (HOMO) and the lowest unoccupied molecular orbital (LUMO). Band gap values are commonly given in electronvolts eV (a non-SI unit).

The sun's radiation is strongest in the visible part oft the electromagnetic spectrum, ranging approximately from 400 nm to 700 nm or 3.1 and 1.8 eV (for spectrum see figure 2). Therefore, the material's band gap also has to be in this energy range to be suitable for PV technologies. Additionally, the band gap defines the photovoltage which can be achieved with a certain material. A smaller band gap means more photons can be used to excite electrons and lead to a higher J_{SC}, but results in a decrease of the highest achievable voltage of the device.

Typically, doped silicon is known for its use as an active material since it fulfills the necessary optical criteria suitable for absorbing sunlight. Nevertheless, more and more other materials, such as conjugated polymers or perovskites, are becoming more popular. Therefore, it is hardly surprising that many different types of solar cells have been realized in scientific communities over the past years and are currently extensively researched [3, 45].

In a solar cell the active material is basically sandwiched between the electrode material. The active material absorbs light and uses the additional energy for electrical processes. Silicon has been used in solar cells for a long time and is a very common material for commercially available PV technologies. In 2014 92% of the total photovoltaics production was silicon wafer based [11]. Such devices consist of two layers of doped silicon. A n-type layer and a usually thicker p-type layer, that can be doped with boron group elements and nitrogen group elements, respectively. Its simplified physical features and its electron transport process is depicted in figure 5a [25]. The electron-hole-pair is created in the p-layer and after it's separation the electron moves along an energetic slope towards the positive electrode.

Comparably new instead are organic solar cells based on conjugated polymers, other organic molecules, and fullerene derivatives like [6,6]-phenyl-C_{61}butyric acid methyl ester (PCBM). Here, an electron donor-acceptor model is used to describe processes in the solar cell (see figure 5b) [25]. Similarly hybrid solar cells can be described with the donor-acceptor model, since conjugated polymers can donate electrons which can be accepted by certain inorganic semiconducting materials. Additionally, photoinduced charge-carrier generation can occur directly in these materials.

Organic or hybrid solar cells can be assembled by many different materials and in several ways, varying from simple layered stacking to a bulky interweaved structure. The way they are assembled is described as architecture by which solar cells can be categorized.

Three important architectures are shown in figure 6. In a bilayer cell (A) a donor and an acceptor phase are stacked together. As the diffusion length of an exciton is rather short (limited to 10 nm [7]) it must be generated close to the layer interface. A planar bilayer setting has a very limited area, where this can happen. Nanostructured bilayer settings (B) can

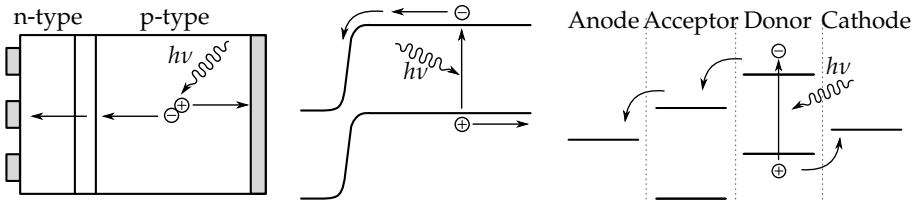

(A) Crystalline silicon solar cell. On the left hand side the physical features are shown. The p-type layer is usually thicker, hence most light is absorbed in this part. The white part between the silicon layers is the junction area, the grey areas are cathode and anode. On the right hand side the electron transport process is depicted.

(B) Electron transport process in a donor-acceptor model.

FIGURE 5: Basic features and electron transport processes of a doped inorganic semiconductor system and a donor-acceptor model (as in organic or hybrid solar cells). [25]

increase the interfacial area, although it is a challenge to produce ordered nanostructures in suitable sizes (a view tens of nanometers). Avoiding complicated processes but increasing the interfacial area can be achieved with a bulk heterojunction (BHJ) architecture (C) and this is therefore a very commonly used architecture [9, 12, 34, 42, 44, 46]. The donor and the acceptor material is usually premixed and then coated on a substrate, whereby an interweaved structure is obtained.

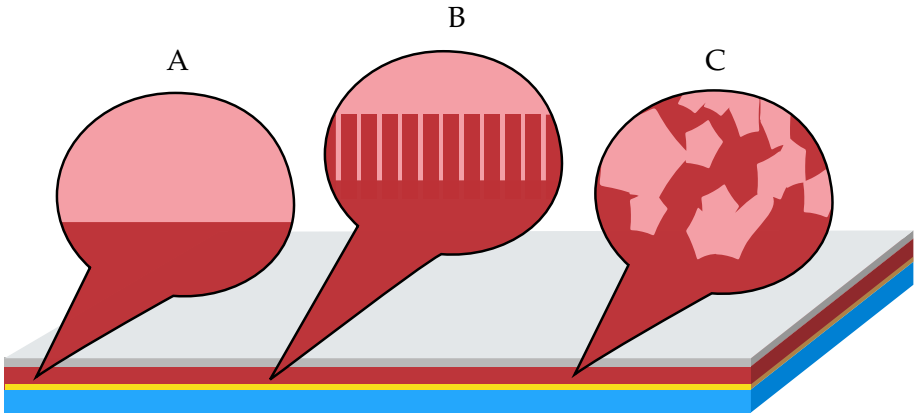

FIGURE 6: Solar cells architectures. The cell is built on glass (bottom, blue) coated with ITO (yellow), the active material is in-between (red), and on top is a second electrode (grey). *A* shows the a simple bilayer heterojunction stacking, *B* a nanostructured active material, and *C* a bulk heterojunction active material.

2.3 SOLAR CELL CHARACTERISTICS

2.3.1 *Ideal Characteristics*

Solar cells to which a varying voltage is applied produce a certain current. Therefore they can be characterized via the relation between voltage and current, shown in figure 7a. The corresponding I-V characteristics can be described by the Shockley solar cell equation [25].

$$I = I_{ph} - I_0 \left(e^{\frac{qV}{k_B T}} \right) \tag{1}$$

In this equation the current I is defined as the difference between the photogenerated current I_{ph} and the saturation current times an exponential term including the electron charge q, the voltage V, the Boltzmann constant k_B and the temperature T. The saturation current I_0 indicates that a non-illuminated solar cell functions as a diode. The I_{ph} is usually independent of the voltage. Ideally I_{ph} is equal to the short circuit current I_{SC} and the open circuit voltage V_{OC} can be defined as

$$V_{OC} = \frac{k_B T}{q} ln \left(1 + \frac{I_{ph}}{I_0} \right) \tag{2}$$

Further the maximum power P_{max} (maximum power point, MPP, figure 7b) of a cell is given according to $P = IV$ at I_{MPP} and V_{MPP}. The fill factor (FF) is calculated by equation 3. The power rectangle $V_{MPP} * I_{MPP}$ approaches the rectangle of $V_{OC} * I_{SC}$ with increasing FF and more power can be produced by the solar cell. The power rectangle is depicted green in figure 7a)

$$FF = \frac{P_{max}}{V_{OC}\ I_{SC}} = \frac{V_{MPP}\ I_{MPP}}{V_{OC}\ I_{SC}} \tag{3}$$

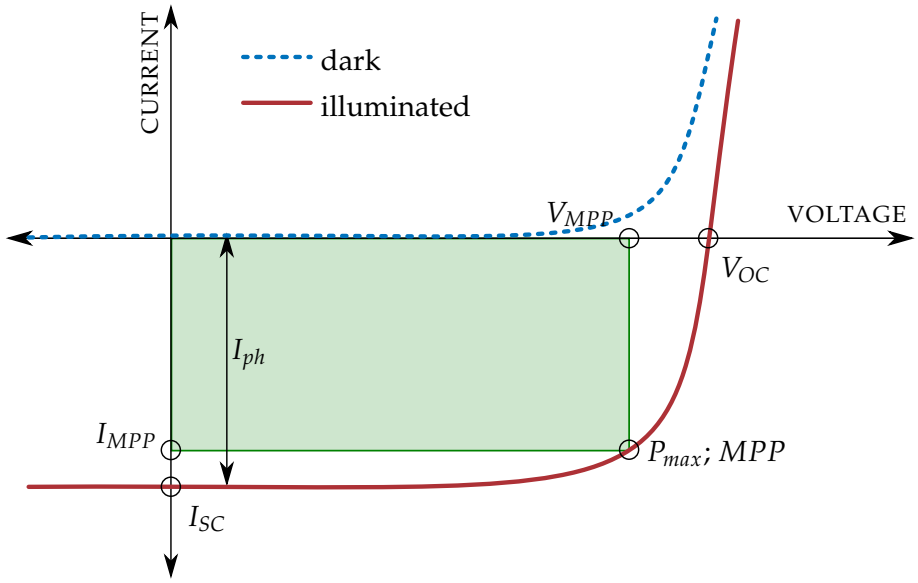

(A) I-V characteristics.

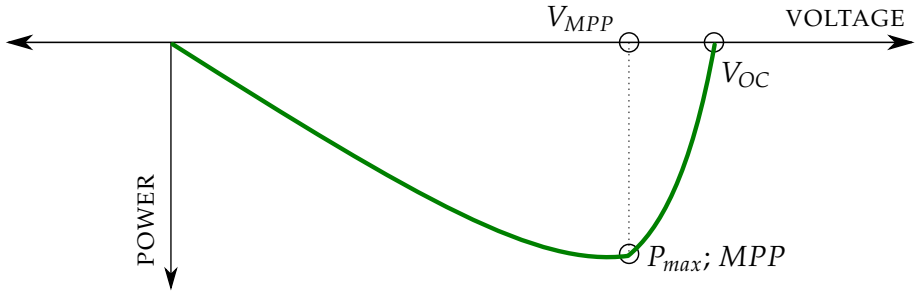

(B) P-V characterisitics.

FIGURE 7: The I-V characteristics compared to the P-V characteristics of an ideal solar cell.

2.3.2 *Solar Cells in Practice*

A solar cell behaves like a diode in the dark. Contrary to ideal cells I_{ph} depends on the voltage for real solar cells. To describe the voltage-dependent behavior the so called two- or double-diode model can be used with some limitations (figure 8). It assumes an ideality factor n which is a function of the voltage. At high voltages the behavior is nearly ideal and $n = 1$. Recombination is dominated by the surfaces and bulk regions. The ideality factor approaches two at lower voltages and the recombination is dominated in the junction. This behavior is modeled with adding a second diode (with $n = 2$). Additionally, shunt (parallel) and

series resistances must be taken into account for real cells. Their effects on the ideal I-V characteristics are schematically shown in figure 9.

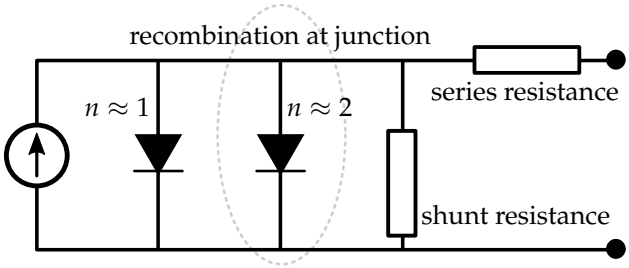

FIGURE 8: A simple scheme of the double-diode model [29].

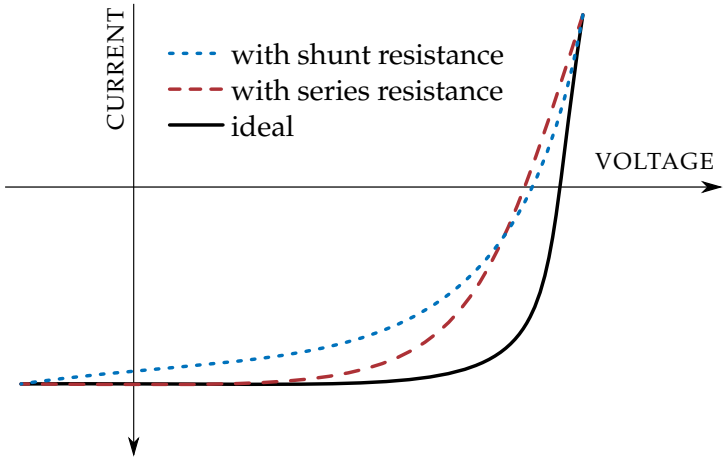

FIGURE 9: The influences of resistances on the I-V characteristics (schematic) [25].

Furthermore the current I is normalized to the area of the cell and expressed as the current density J (usually in mA/cm²), because a bigger area would lead to a higher value for I without any real improvement. This practice makes cells of different shapes and sizes comparable. An important cell parameter is the short circuit current density (J_{SC}).

One of the most commonly used values to compare solar cells is their PCE. It is the fraction of the power which has been generated by the cell (P_{OUT}) over the power of the light source (P_{IN}) and is calculated from the data of I-V measurements via equation 4.

$$PCE = \frac{P_{OUT}}{P_{IN}} = \frac{V_{mpp} * J_{mpp}}{P_{IN}} = \frac{V_{OC} * J_{SC} * FF}{P_{IN}} \tag{4}$$

The quantum efficiency (QE) is the number of electrons generated in the cell and provided to the external circuit per incident photon at a certain wavelength (λ). More precisely, all photons that hit the cell surface are taken into account for the external quantum efficiency (EQE), while only those photons that are not reflected on the surface are taken into account for the internal quantum efficiency (IQE). The mathematical relation between IQE and I_{ph} is shown in equation 5, where $\Phi(\lambda)$ is the incident photon flux on the cell and $R(\lambda)$ is the reflection coefficient at wavelength λ.

$$I_{ph} = q \int_{(\lambda)} \Phi(\lambda) \ \{1 - R(\lambda)\} \ IQE(\lambda) \, d\lambda \tag{5}$$

The EQE of an ideal cell should look as shown in figure 10. Ideally it resembles almost a rectangle, which means a broad spectrum of light is being adsorbed and the produced charge-carriers are successfully collected at the electrodes. In practice the EQE unambiguously differs from a rectangle. It shows similarities to the UV-VIS spectrum of the material. The QE is dependent on the absorption of light and varies further due to recombination and reflections.

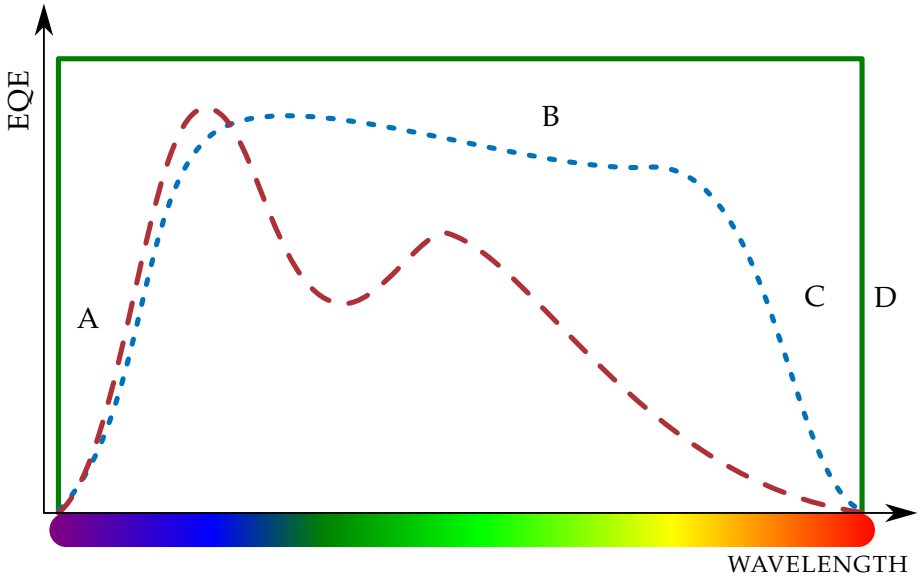

FIGURE 10: EQE diagram. It shows what an EQE could look like: The green (continuous) line depicts an ideal solar cell, the blue (dotted) line a classic inorganic cell, and the red (dashed) line a hybrid solar cell. The deviation of ideal behaviour is due to different absorption of light, in region A due to surface recombinations, in region B (overall) due to reflection and low diffusion length, in region C due to surface recombination and reduced absorption of long wavelengths, and region D where the band gap energy is not reached at this wavelengths. [30].

2.4 HYBRID SOLAR CELLS

2.4.1 *General*

Organic solar cells have become more attractive since their efficiencies increased. This already started with the discovery and development of conductive polymers in the 1970s and finally gained more attention in 2000 with the Nobel Price of Heeger, MacDiarmid, and Shirakawa [15]. More recently it was further accelerated by the crossing of the 10% efficiency mark in 2012 [13, 22].

Hybrid solar cells consist of a semiconducting polymer (donor) and an semiconducting inorganic nanostructured material (acceptor). They keep many advantages of organic cells such as their lightweight, flexible, or transparent properties, a broad absorption of light, and also the possibility of inexpensive roll-to-roll production methods trough printing or coating. Further hybrid solar cells can be modified via tailoring the inorganic phase. Composition, size, and shape can be tuned to change electrical properties, and charge-carrier mobility is increased [33].

In hybrid solar cells inorganic nanomaterials are embedded in a conductive polymer matrix. Among others, examples for such inorganic materials are the commonly used cadmium compounds like cadmium sulfide (CdS), selenide (CdSe) or telluride (CdTe) that lead to comparably high PCEs of 4.1, 3.64, and 3.2%, respectively [4, 18, 35]. Because of their non-toxic and inexpensive properties materials such as titanium dioxide (TiO_2) [44] or zinc oxide (ZnO) [28] are used, as well as copper indium disulfide (CIS) [34].

There are different ways to produce nanocomposite materials. They can be divided into three major synthetic routes [33]. These routes are (*i*) the classical, (*ii*) the infiltration, and lastly (*iii*) the in-situ approach which was used in this work.

(*i*) In a classical approach the nanoparticles are separately synthesized and purified, and then dissolved with the conjugated polymer. This

external synthesis allows to produce very defined nanoparticles in many variations. This is usually not possible with the in-situ approach. However, the classical approach often needs additional steps, such as removing excess capping ligands and ligand exchange. Bulky ligands are used to prevent nanoparticle agglomeration during the processes. They can negatively influence basic and important electrical processes within a solar cell such as charge dissociation and transport so that they have to be exchanged for other ligands, which do not show these effects. However, it has to be taken into account that the exchange of ligands always influences the solubility. Overall, this leads to a higher synthetic effort, which can be avoided chiefly, by the in-situ route.

(*ii*) An infiltration approach is performed when an inorganic nanostructure is pre-formed, which then is infiltrated by the conjugated polymer. These nanostructures can be highly ordered, highly porous or an array of nanorods, and therefore the interfacial area of the polymer-inorganic phase can be increased very specifically. Additionally dead ends of the inorganic phase can be prevented to a large extent. On the downside the infiltration approach is unsuitable for roll-to-roll processes and is therefore more expensive.

(*iii*) The in-situ approach uses nanoparticle-precursors, which are mixed with the conjugated polymer. Then they can be either formed in-situ in solution and coated in a second step, or they can be coated first to obtain a precursor layer, which is then converted to a polymer-nanoparticle hybrid layer. The possibility of inexpensive procedures and low synthetic efforts are the great strengths of this approach. However, this comes with some drawbacks. As the formation of the nanoparticles takes place in the presence of the conjugated polymer, the range of moderate temperatures is limited. The difference in density between precursors and nanoparticles as well as volatile decomposition compounds cause the layer to undergo a significant volume change during the conversion step and has to be taken into account. Further the size of in-situ formed nanoparticles can not

be altered easily. Nevertheless, the in-situ route provides a very elegant method to produce nanocomposite layers for BHJ solar cells.

2.4.2 *Polymer-CIS Solar Cells*

CIS is a semiconducting material with interesting properties utilizable for PV technologies. $CuInS_2$ shows a chalcopyrite structure similar to copper iron disulfide ($CuFeS_2$). It offers a lower band gap compared to CdSe or CdS (1.5 eV, 1.74 eV and 2.4 eV, respectively).

In 2011, Rath et al. [34] introduced an in-situ formation route for CIS nanoparticles in polymer/CIS hybrid solar cells. The CIS nanoparticles were formed from metal xanthate precursors under mild conditions (below 200 °C). The formation temperatures can be lowered to 140 °C by adding n-hexylamine. This was done to produce a polymer/CIS absorber layer on a plastic substrate to produce flexible devices (investigated by Fradler et al. [10]). The lower temperature also had a positive influence on the device stability. Further, the polymer/CIS ratio is of great importance. Arar et al. [1] studied weight ratios from 1:3 to 1:15. They achieved the best morphologies with a 1:9 polymer/CIS weight ratio. The architecture of polymer/CIS solar cells in connection with the top-electrode material and the stability was investigated by Dunst [8]. The exchange of aluminum for silver as the electrode material increased the stability drastically. However, a lower V_{OC} was observed compared to devices with aluminum electrodes. The introduction of a TiO_x interlayer helped to increase the V_{OC} of devices with silver electrodes and stabilized devices with aluminum electrodes. So called *inverted* architecture devices ITO | TiO_x | absorber-layer | PEDOT:PSS | Ag were realized.

In this work the *in-situ* route was applied to produce the CIS nanoparticles. In contrast to a route, where the nanoparticles are synthesized separately and then introduced into the polymer, the CIS particles are directly produced in the polymer matrix from metal xanthate precursors (figures 11a and 11b) via heat treatment. The polymer and

copper and indium xanthates were well dissolved and applied on the substrate. At temperatures of 145 °C to 195 °C the CIS nanoparticles were formed in the polymer and solvent residues and volatile reaction byproducts were removed during the heat treatment. This process could be visually observed in the change of color from violet to brown, when polymer-precursor layer converts to a polymer-CIS layer.

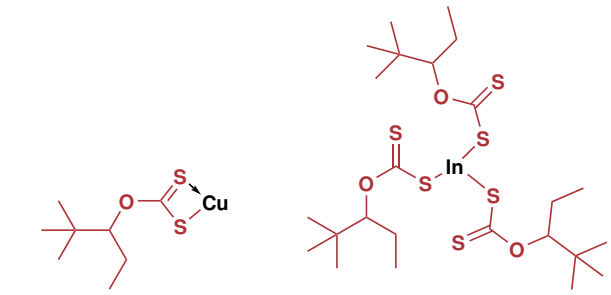

(A) Copper(I) O-2,2-dimethylpentan-3-yl dithiocarbonate

(B) Indium(III) O-2,2-dimethylpentan-3-yl dithiocarbonate

FIGURE 11: Copper and indium metal xanthates are precursors for CIS nanoparticles.

The applied reaction is the Chugaev elimination, named after Lev A. Chugaev (or *german*: Tschugaeff). He described xanthates in his studies on the thujone [43] in 1900. In general, in the Chugaev elimination alcohols react with carbon disulfide (CS_2) to alkenes. The intermediate is a xanthate – usually referring to a compound with the general formula $R^1OCS_2R^2$ or the salt $ROCS_2{}^-M^+$. The elimination reaction is depicted in figure 12.

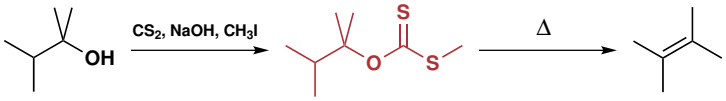

FIGURE 12: Chugaev elimination reaction. The xanthate intermediate in the middle (red).

Advantages of such an *in-situ* route that uses xanthates to produce inorganic sulfide nanoparticles can be seen quite clearly. The xanthates with apolar alkyl groups are soluble in many organic solvents, the metal is bound by the sulfur atoms, which serves as sulfur source to form the CIS

particles. The volatile byproducts are evaporated out of the composite layer. This allows cost efficient production.

The ratio of copper and indium is crucial for the use in PV devices. A surplus of indium forms a n-type semiconducting material whereas a surplus of copper does the opposite and a p-type material is formed [21]. The n-type is needed for polymer-CIS hybrid solar cells. A previous publication showed a copper indium ratio of 1:1.7 led to the best results [1].

3

THE AIM OF THIS THESIS

Polymer-nanoparticle hybrid solar cells combine advantages of organic and inorganic materials in an elegant way in one device. Besides advantages due to the easy processability of polymers, both phases can function as active material itself and broaden therefore the absorbed spectrum of the light. Copper indium sulfide (CIS) is an attractive inorganic semiconducting material for the application in hybrid solar cells due to its optical and electronic properties. In several recent studies polymer/CIS hybrid cells have already been investigated and power conversion efficiencies up to 3% have been realized. However, the potential of polymer-CIS hybrid cells is not fully exploited yet.

Previous studies focused for example on the CIS nanoparticle synthesis and the introduction of the nanoparticles in the absorber layer. Thereby, a method in which the CIS nanoparticles are prepared from solution in an in-situ approach directly within the conjugated polymer from metal xanthates was developed. Topics, like e.g. the influence of processing conditions or the CIS content on the solar cell performance, morphology, electrode materials and device stability have been already investigated [1, 8, 10, 16, 34]. However, the influence of different conjugated polymers or the influence of or organic molecules as modifiers of the polymer/nanoparticle interface has not been extensively investigated yet. Therefore, this thesis focuses on these topics.

PCDTBT, a conjugated polymer, was used to investigate the CIS content and the influence of the coating technique (doctor blading, spin coating). Additional focus was set on testing polymers with different molecular weight. A high molecular weight can influence the morphology of the layer to benefit the cell performance.

Also small polar organic molecules used as additives can enhance the performance of organic or hybrid solar cells [12]. It is possible that these molecules modify the microstructure of the nanoparticles or the interface between polymer and nanoparticles. Therefore, benzene-1,3-dithiol, pyridine, and 1,8-diiodooctane were investigated. Facile methods to introduce them into the active layer were evaluated in terms of the PCE. These methods included adding the molecules directly into the solution or treating the absorber layer with the polar molecule.

In other studies, very high efficiencies were achieved with the polymer PffBT4T-2OD. This conjugated polymer showed efficiencies higher 10% in combination with a fullerene derivative [23]. Therefore, experiments to investigate the potential of this material in combination with inorganic CIS nanoparticles have been also performed within this thesis.

PPDTBT is a conjugated polymer rather new for organic or hybrid solar cells. It shows similarities to PCDTBT. Knowledge generated from experiments with PCDTBT-CIS hybrid solar cells was used and applied to the experiments with PPDTBT.

Part II

RESULTS AND DISCUSSION

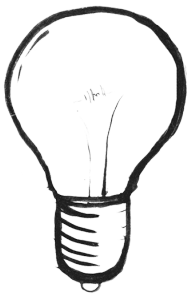

4

PCDTBT/CIS SOLAR CELLS

In this thesis mainly the conjugated polymer poly[N-9'-heptadecanyl-2,7-carbazole-alt-5,5-(4,7-di-2-thienyl-2',1',3'-benzothiadiazole)], abbreviated PCDTBT, was used for polymer/CIS hybrid solar cells. The structure is shown in figure 30.

The potential of hybrid solar cells with materials such as PCDTBT-copper indium disulfide (CIS) is not fully investigated yet. The morphology, the polymer/nanoparticle ratio, the layer thickness, the surface and additive treatment ot the manufacturing processes can be varied to enhance the solar cell performance. This leads to a high sensitivity of the cells towards their environment during assembling and is challenging in terms of reproducability. Therefore, facile and quick procedures with few steps should be investigated to produce sound methods for solar cell production.

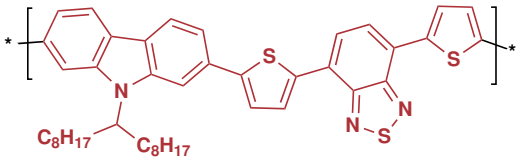

FIGURE 13: The structure of the conjugated polymer PCDTBT.

The PCDTBT/CIS active layer was applied using two different casting methods: Doctor blading which has already been used in other studies of polymer/CIS hybrid solar cells [1, 8, 10], and casting by spin coating that promises high variability.

A surplus of indium was used in a Cu:In ratio of 1:1.7 to produce a n-type semiconductor material. This is necessary in a system with a donor polymer. Due to the density of CIS a weight ratio of 1:4.3 of organic and inorganic phase, respectively, leads to a volume ratio of approximately 1:1 or 50 vol% inorganic phase [47]. This ratio could be assumed to be preferable, because both phases are well balanced. In the study of Arar et al.

the best efficiency was achieved by cells with a weight ratio of 1:9 (which corresponds approximately to 68 vol% CIS).

Further, Arar et al. [1] investigated the layer morphology by transmission electron microscopy (TEM). Three different nanoparticle loadings (1:3 or 41 vol%, 1:9 or 68 vol%, 1:15 or 78 vol%, weight ratio or vol% CIS, respectively) were investigated and it was found that the particles tend to agglomerate with higher CIS contents. It is suggested that this agglomeration also causes the polymer phase to expand and could prevent exciton dissociation.

Moreover, selected area electron diffraction (SAED) patterns of layers containing different CIS loadings revealed that the nanoparticles have the same crystallinity and crystal structure. A size of approximately 3 nm for each sample was measured by TEM, which suggests equal charge carrier mobilities in the CIS phase for different CIS loadings.

In a solution containing the polymer and the metal xanthates, the amounts of metal xanthates were calculated for desired CIS loadings in the finalized layer using the density of CIS nanoparticles and the polymer concentration.

4.1 CIS CONTENT AND LAYER THICKNESS

The first experiments in this work were performed with a low molecular weight (Mw) polymer using doctor blading. The CIS content was varied from around 40 vol% to 80 vol%. Very quickly good efficiencies were achieved and the results showed a trend for optimum CIS loadings.

It was observed that the efficiency increased with a higher amount of inorganic phase until reaching 68.5 vol% CIS. This corresponds to a polymer/CIS weight ratio of 1:9.33. Significantly affected by the CIS content was the J_{SC} with an increase from 2.46 $\pm$ 0.18 mA/cm² (38 vol% CIS) to 8.01 $\pm$ 0.49 mA/cm² (68.5 vol% CIS). Equally, the FF reaches the maximum value at 68.5% CIS (59.2 $\pm$ 1.0 %). The V_{OC} was similar around 40 vol% to 50 vol% (0.43 $\pm$ 0.01 V), increases just slightly for 68.5 vol% and decreases for 79 vol% CIS (0.46 $\pm$ 0.02 V). These trends are illustrated in

figure 14. The average cell parameters for the five best cells can be found in table 1.

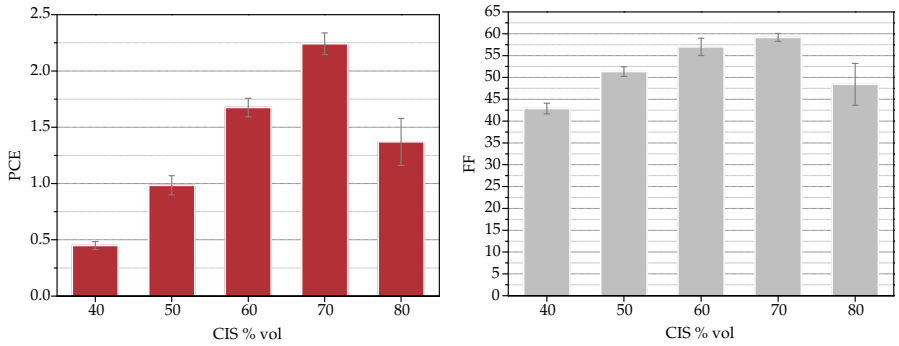

(A) Compared PCE (B) Compared FF.

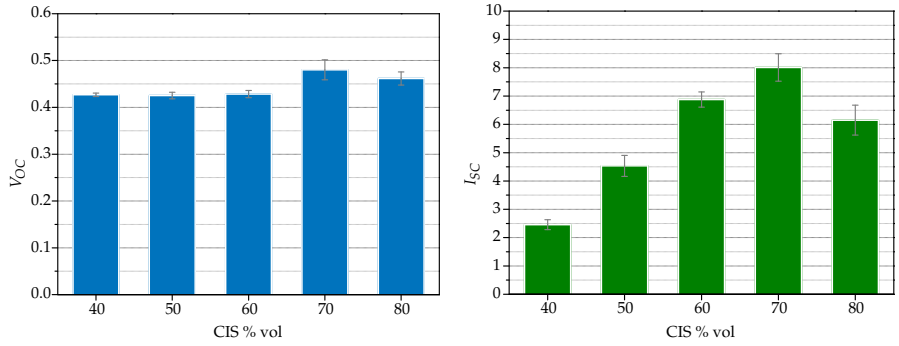

(C) Compared V_{OC}. (D) Compared J_{SC}.

FIGURE 14: Comparison of the five solar cells with the highest PCE, each with a different CIS content (in vol% after the heat treatment).

TABLE 1: Averaged solar cell parameters of the five PCDTBT/CIS cells with the highest PCE for each CIS content. The cells are built using doctor blading.

CIS [vol%]	V_{OC} [V]	J_{SC} [mA/cm²]	FF [%]	PCE [%]
38	0.43 ± 0.01	2.46 ± 0.18	42.9 ± 1.3	0.45 ± 0.04
48	0.43 ± 0.01	4.53 ± 0.37	51.3 ± 1.2	0.98 ± 0.09
58	0.43 ± 0.01	6.88 ± 0.27	57.0 ± 2.0	1.67 ± 0.09
68.5	0.48 ± 0.03	8.01 ± 0.49	59.2 ± 1.0	2.24 ± 0.10
78.8	0.46 ± 0.02	6.15 ± 0.53	48.4 ± 4.8	1.37 ± 0.21

Doctor bladed at 40°C, 7.5 mm/s. $n = 5$.

Additionally, not only the best five solar cells, but all working cells were evaluated. For PCE and V_{OC} the trend, that the highest values are obtained with samples having approximately 68.5 vol% CIS, is still valid. In figure 15

the average values for the solar cell parameters are presented as light grey bars, while the maximum value is presented as green bars. It shows that a slightly higher FF was achieved with 48 vol% CIS (15b). For the parameter J_{SC} the maximum, as well as the average value of all devices was higher for 58 vol% than for 68.5 vol% CIS. Nevertheless, at 68.5 vol% CIS the PCE was always the highest and the standard deviations were comparably small.

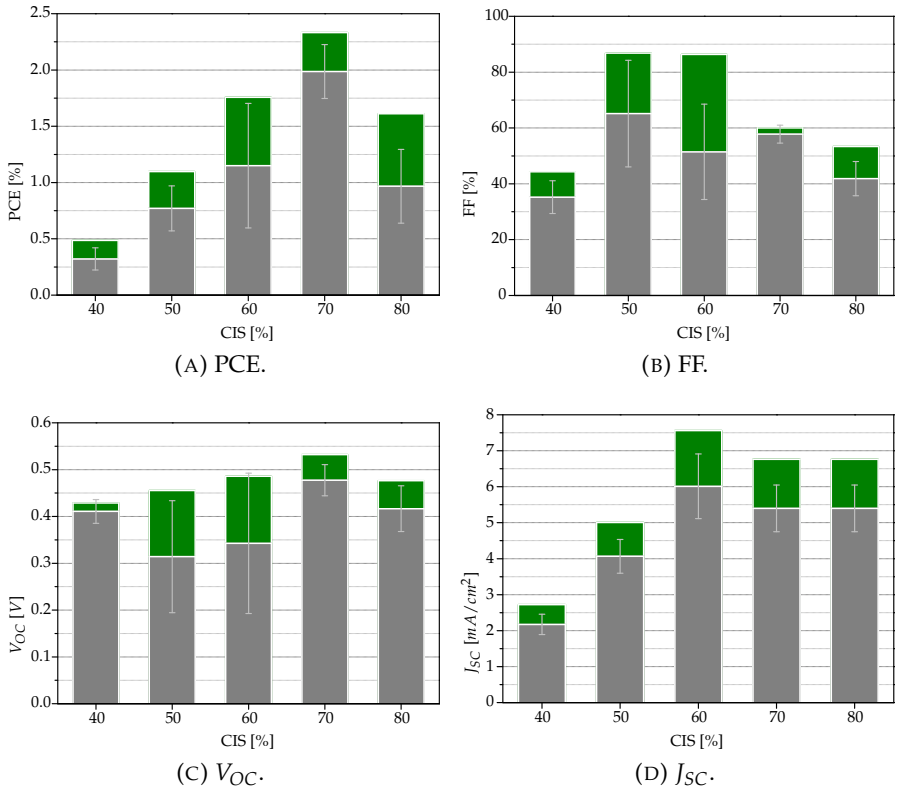

(A) PCE. (B) FF.

(C) V_{OC}. (D) J_{SC}.

FIGURE 15: Comparison of solar cell parameters for all working cells on the substrate with different CIS content in the heat treated layer. The grey bars show the average values, while the (higher) green bars represent the highest achieved value.

Aside from solar cell parameters the film thickness of the devices was measured. It emerged that the difference in CIS loading heavily influenced the resulting film thickness. When all layers were prepared with the same doctor blading parameters no equally thick layer could be obtained because of the different CIS loadings. For devices with CIS content of 58 vol%, 69 vol%, and 79 vol% the thickness increased from approximately 50 nm to 102 nm (see table 2).

TABLE 2: Absorber layer film thicknesses (prepared via doctor blading) of solar cells compared with CIS nanoparticle loading using low Mw PCDTBT

CIS	THICKNESS*	ROUGHNESS	PARAMETERS	
[vol%]	[nm]	[nm]	V_{OC} [V]	J_{SC} [mA/cm²]
58	51 ± 5	1.8 ± 1	0.43	6.9
69	74 ± 6	1.8 ± 1	0.48	8.0
79	102 ± 8	2.0 ± 1	0.46	6.2

The average PEDOT:PSS layer for doctor blading was 33 nm thick.

Organic BHJ solar cells with a layer of polymer-PCBM blend struggle with low charge-carrier mobility and limited diffusion lengths which leads to high probabilities of charge-carrier recombination [6, 14, 17]. This also applies partly to nanocomposite cells with inorganic nanoparticles in a conjugated polymer. Therefore, the layer thickness is of great importance – especially for PCDTBT which has comparatively low charge-carrier mobility [23] of $6 * 10^{-5}$ cm²/Vs [38]. This at least two magnitudes lower than the mobility in other conjugated polymers such as P3HT or PffBT4T-2OD (for full names see section 8.1).

Namkoong et al. [26] investigated PCDTBT/PCBM solar cells with regards to their layer thickness. Similar to the observations made in this study they quoted reports of decreasing efficiency with increasing layer thickness and a maxumim efficiency with a photoactive layer thickness of 70 to 90 nm [27, 42]. The experiments they performed with PCDTBT-$PC_{71}BM$ (70 to 150 nm), supported these results as cells with 70 nm lead to the highest PCE of 6.5%. The PCE decreased with elevated layer thickness (4.7% at 133 nm), but increased again at 150 nm to 5.02%. The increasing PCE with higher film thickness can also originate from certain optical effects within the layer, such as internal

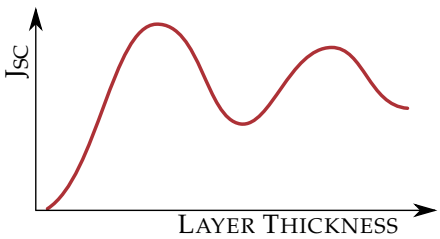

FIGURE 16: Two mamxima of J_{SC} vs the film thickness.

reflections. Many times a second maximum occurs, as shown in figure 16 for the J_{SC}.

Higher molecular weights of the conjugated polymer normally promise a higher charge-carrier mobility and also changes in morphology of the polymer/nanoparticle layer can be expected. A possible positive influence on the performance of PCDTBT/CIS solar cells was investigated. However, the preparation in general had to be adapted for the high molecular weight polymer. The low Mw polymer was easily soluble in chlorobenzene (CB) at room temperature, whereas the high Mw polymer needed elevated temperatures above 75 °C in order to be dissolved completely. To prevent big changes in the solution concentration trough evaporation dichlorobenzene (DCB) was used, either pure or in a 1+1 mixture with CB. Additionally, PCDTBT is better soluble in CDB. The lower vapor pressure of DCB, however, causes long processing times when doctor blading is used. In general, PCDTBT dissolved in CB resulted in significantly higher layer thickness, while adding DCB made the layers thinner. To easily vary the film thickness spin coating was used to apply the active material.

Spin coated layers were found to vary strongly in thickness. The thickness was dependent also on the amount of CIS precursors in the solution, which influenced the viscosity. In the beginning the layer thickness was significantly too high. Changing the rotation speed alone was not enough to control the thickness. Therefore, dilution was used as a helpful method to vary the thickness. Additionally it made the surfaces more smooth.

CIS loadings from 48 vol% to 79 vol% in high Mw PCDTBT have been investigated in relation to the film thickness. As an overview measurement results are presented in figure 17. More data is listed in table 3. Similar to the low Mw, in this series of experiments, PCDTBT solar cells with approximately 70 vol% CIS showed the highest PCE of 2.08%. However, by using high Mw PCDTBT no clear improvement could be observed in the overall performance.

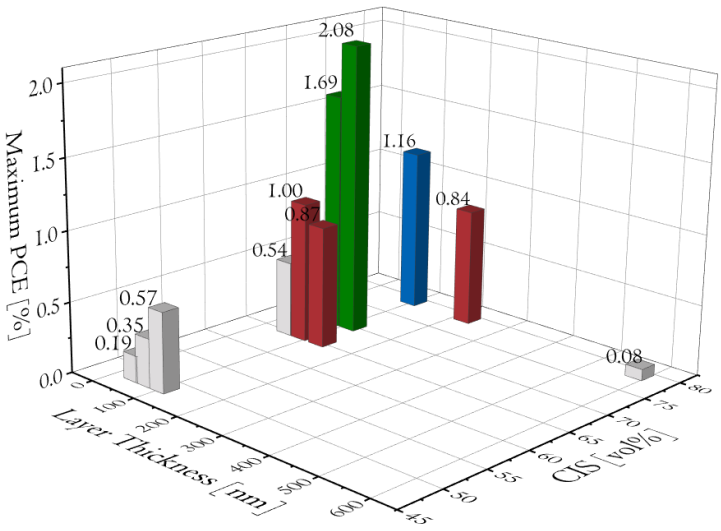

FIGURE 17: The layer thickness (y-axis, bottom left hand side) with the volume of CIS in the heat treated layer (x-axis, bottom right hand side) vs. the PCE of the best cell (z-axis). Column color: green PCE > 1.5%, blue PCE > 1%, red PCE > 0.5%, grey PCE < 0.5.

TABLE 3: PCE, layer thickness, roughness, and parameters of solar cells with different CIS loadings and high Mw PCDTBT.

PCE*	THICKNESS	ROUGHNESS	PARAMETERS		
[%]	[nm]	[nm]	V_{OC} [V]	J_{SC} [mA/cm²]	FF [%]
		48 vol% CIS			
0.57	103 ± 3	≤ 1	0.54	2.79	38.0
0.35	70 ± 3	≤ 1	0.51	1.67	41.1
0.19	41 ± 6	≤ 1	0.43	0.96	45.4
		65 vol% CIS			
0.87	130 ± 11	7.5± 0.7	0.51	4.02	42.7
1.00	89 ± 9	≤ 1	0.54	4.05	46.3
0.54	54 ± 2	≤ 1	0.48	2.35	47.5
		70 vol% CIS			
2.08	113 ± 8	1.3 ± 0.6	0.54	9.94	
1.69	78 ± 7	1.3 ± 0.6	0.51	8.76	
		79 vol% CIS			
0.08	586 ± 66	10.3 ± 9	0.16	1.41	35.1
0.84	223 ± 17	2.7 ± 1	0.46	4.19	44.5
1.16	99 ± 4	1.3 ± 0.6	0.45	4.88	49.4

* Of the solar cell with highest value.

The layer thickness of the tested solar cells with the concentration of the used solution are shown in figure 18a. A CIS content of 70 vol%, using a 5 mg/ml polymer solution, led to the device with the highest PCE in this series (see table 3). The device absorber layer thickness of 113 nm is drawn as a black dotted line in figure 18a for comparison. This layer was significantly thicker than the one with lower Mw (74 nm). A thinner layer of 78 nm decreased the PCE further.

A CIS loading of 79 vol% and a 5 mg/ml solution resulted in an extremely thick layer. Dilutions of 2+1 and 1+1 led to a thickness decrease of 60% and 80%, and resulted in PCEs of 0.84% and 1.16%. The thinnest layer for 79 vol% had a thickness of 99 nm. With 65 vol% CIS and a thickness of 89 nm a PCE of 1% was measured.

The evaluated data clearly point to a optimal thickness of 90 nm to 115 nm for high Mw PCDTBT/CIS solar cells (figure 18b).

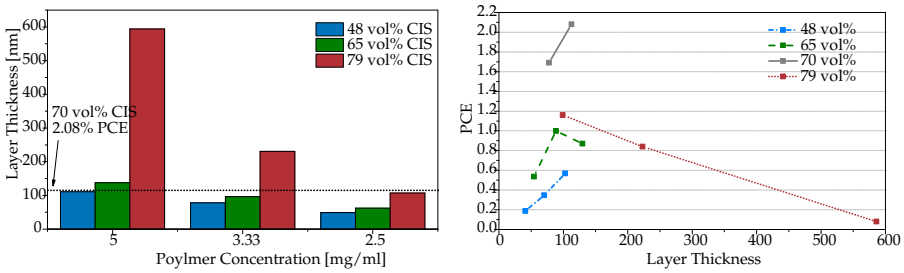

(A) Varying layer thickness of PCDTBT/CIS with different solution concentrations..

(B) The PCE correlated to the film thickness.

FIGURE 18: Film thickness of PCDTBT/CIS solar cells and PCE.

Applying active material with the high Mw polymer proved to be challenging, as particles of the polymer tend to precipitate when dropped onto the substrate. This did happen more rarely, when a lower amount of CIS precursor was used. Therefore also low-CIS layers were prepared, which resulted without exception in very even and smooth layers, but the amount of 48 vol% CIS was simply too low to result in well performing solar cells.

UV-VIS spectra were measured for different PCDTBT/CIS layers. In figure 19 two spectra are shown. Higher CIS content increased the absorption

at the local minimum (approximately 475 nm) and between the local maximum (approximately 585 nm) and 1000 nm. The local maximum is not influenced, as it originates from polymer absorption.

The spectra of a high and a low Mw PCDTBT/CIS layer in a range from 400 nm to 1000 nm showed no noticeable difference in absorption. Figure 20 shows the spectra normalized to the layer thickness. This could be a reason for the observation that the higher Mw alone did not increase the PCE.

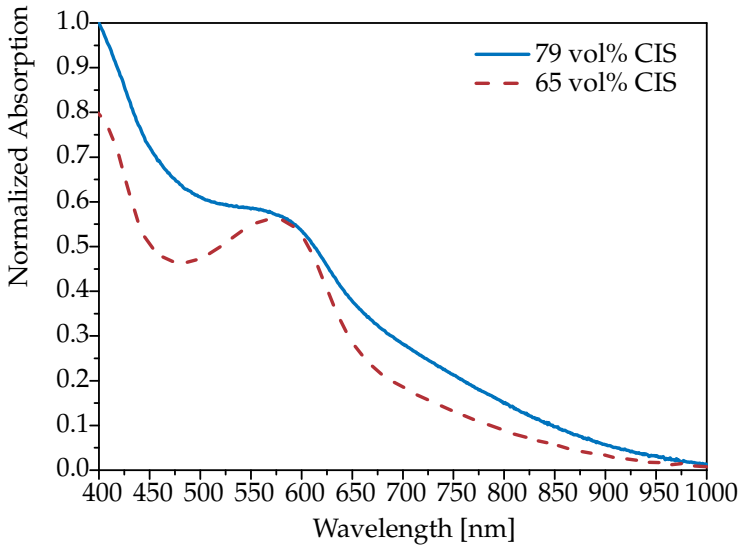

FIGURE 19: Normalized UV-Vis spectra of PCDTBT/CIS with different CIS contents.

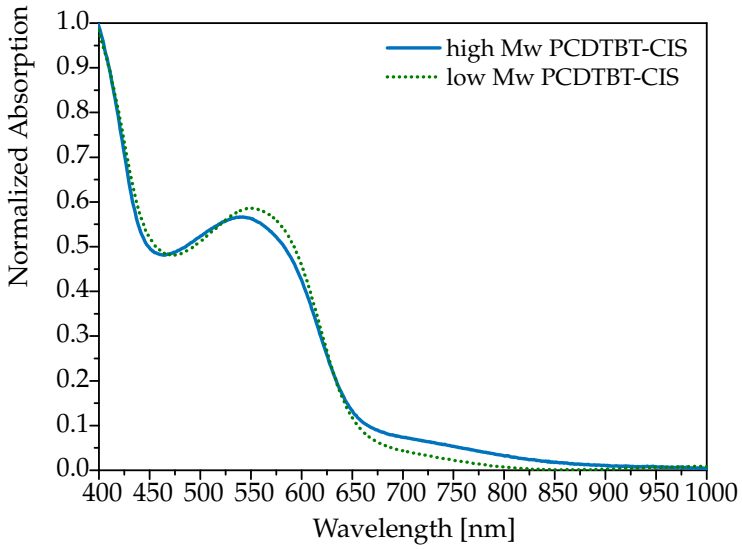

FIGURE 20: The normalized UV-Vis spectra of PCDTBT and 70 vol% CIS and two different molecular weights.

4.2 INFLUENCE OF THE PEDOT:PSS LAYER

A PEDOT:PSS layer was applied via spin coating from solution in two different dilutions. One time an aqueous solution (Heraeus Clevios™ 4083) was used directly, another time it was diluted with deionized water 1+1. All cells were built with 69 vol% CIS from a 5 mg PCDTBT/ml solution. Using the diluted solution slightly higher average values for PCE, FF, V_{OC} and J_{SC} with small deviation could be observed in this series. Nevertheless, the maximum values for PCE, FF and V_{OC} have been observed with pure Clevios™ 4083. Only the J_{SC} seems to be higher for diluted PEDOT:PSS solution on average and maximum. The results are given in table 4.

8 nm is rather thin for a PEDOT:PSS layer but it was observed that these layers were more evenly distributed over the whole substrate. On the other hand 33 nm is a value that can be assumed as suitable for PCDTBT-CIS solar cells.

TABLE 4: Characteristic parameters of PCDTBT solar cells bearing PEDOT:PSS layers prepared from undiluted and diluted PEDOT:PSS solution.

	Undiluted		Diluted	
	AVERAGE	MAX.	AVERAGE	MAX.
V_{OC} $[mV]$	0.37 ± 0.15	0.51	0.41 ± 0.07	0.46
J_{SC} $[mA/cm^2]$	3.10 ± 0.26	3.43	3.22 ± 0.24	3.64
FF [%]	38.2 ± 9.4	47.9	38.8 ± 4.4	42.3
PCE [%]	0.48 ± 0.27	0.80	0.51 ± 0.13	0.64
Thickness	33.0 ± 3.3 nm		8.5 ± 2.4 nm	

$n = 12$ for Heraeus Clevios™; $n = 11$ for diluted solution.

4.3 PCDTBT-CIS LAYER SURFACE

Spin coated photoactive layers applied in a single layer often contained cracks. An image from an optical microscope of a layer containing a very high excess of CIS is shown in figure 21a. It reveals that the polymer is

in this case incapable of avoiding crack formation. Even with lower CIS loadings such cracks have been observed for some samples.

While doctor bladed layers did not show such cracks they occurred frequently in spin coated layers. Even more frequently if applied in a single, rather thick layer (see figure 21b). The application of thinner layers reduced cracks and to compensate for a loss in thickness the layer was applied twice. The quality of the layers was significantly improved, no cracks occurred and it seemed that the organic-inorganic phase distribution was very even. Overall, this led to an improvement of the cell parameters. AFM images of a single layer (with crack) and a double layer are shown in figure 22.

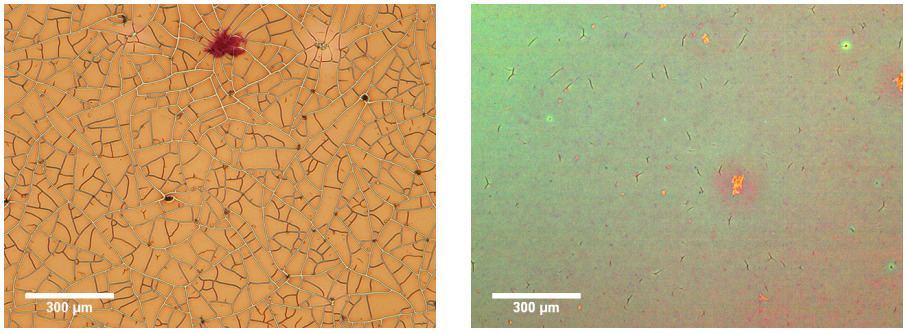

(A) Thick PCDTBT-CIS layer with a high excess of CIS.

(B) Spin coated layer showing small cracks.

FIGURE 21: Cracks in spin coated PCDTBT-CIS layers. In (A) with an excess of CIS, in (B) with normal CIS loadings.

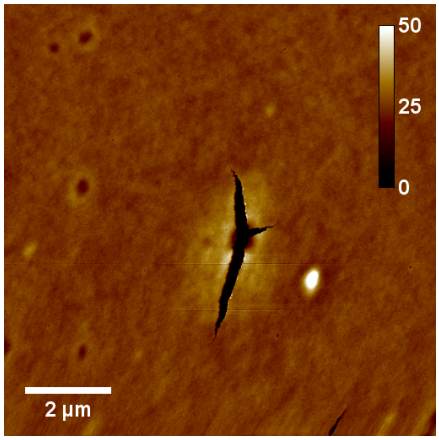

(A) Topographic image: Layer spin coated in one step.

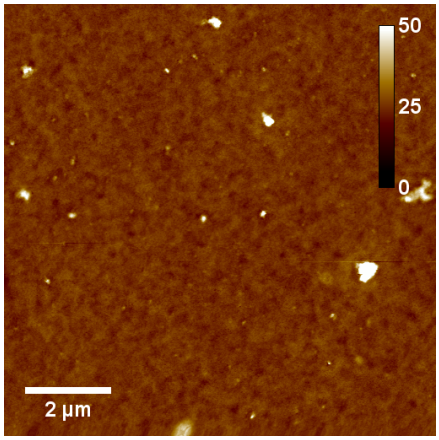

(B) Topographic image: Layer spin coated in two steps and 1+1 dilution.

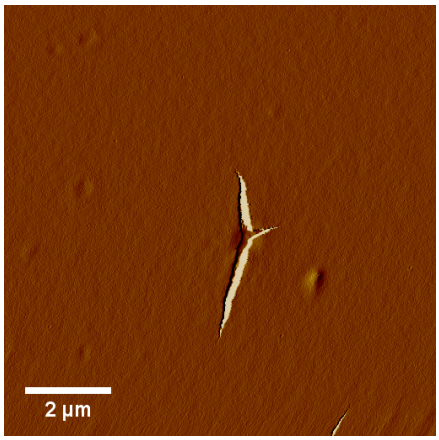

(C) Corresponding phase image to image A.

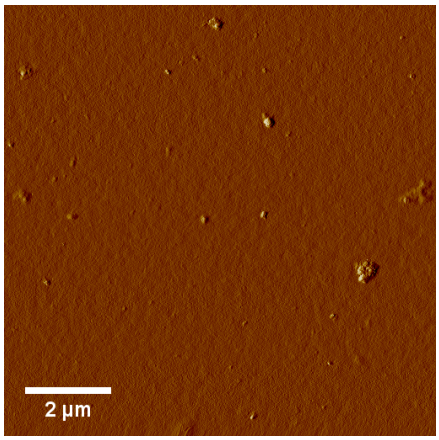

(D) Corresponding phase image to image B.

FIGURE 22: AFM images of two substrates with PCDTBT-CIS (70 vol%) films.

First, the devices were built with TiO_x/Ag electrodes. The devices had good average parameters with V_{OC} values over 0.40 V, J_{SC} values over 6 mA/cm² and FF over 50 (n = 75). Titanium was evaporated in a thin layer onto the substrates without inert gas atmosphere (residual air). This led to the formation of TiO_x [9]. However, this procedure entails inconsistencies of production conditions. Additionally titanium could sometimes not be evaporated with a sufficient thickness via the used equipment. All this led to a low reproducibility. Aluminum, is a less expensive alternative to titanium and silver and has further the advantage of a possible higher voltage due to its work function.

It was observed that using pure silver as electrode material had the advantages of very predictable evaporation behavior. It allowed slow and regular evaporation onto the substrates with stable rates of 0.1 to 5.0 Å/s, which was not the case for aluminum. Silver is more resistant against oxidation than aluminum and devices with silver electrodes were still functional after a few days of storage.

The solar cell with the highest PCE in this study was produced with a silver electrode and its J-V characteristic is shown in figure 23. It achieved 2.46 % PCE, a very high J_{SC} for PCDTBT-CIS devices of 11.2 mA/cm², a good FF of 51 % and a comparably normal but still good V_{OC} of 0.43 V.

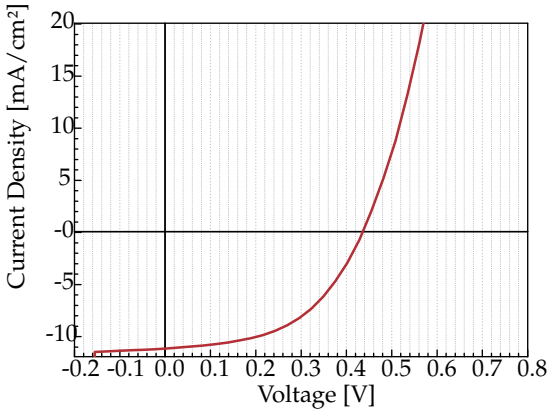

FIGURE 23: Illuminated J-V curve of a device with Ag-electrode and 2.45% PCE.

4.5 EXPOSURE TO AIR

It was observed that PCDTBT/CIS solar cells increased in efficiency when they were exposed to air. The most efficient cells built using doctor blading had titanium oxide intermediate layers (glass | ITO | PEDOT:PSS | PCDTBT/CIS | TiO_x | Al). These were applied by thermal evaporation after a simple transfer through normal room atmosphere. Similarly, other cells improved by simply exposing them to air after they were built. Therefore, investigations under more controlled circumstances were performed.

It was determined at which step in the fabrication process the exposure had the best effect on the solar cell parameters. For all devices the best results were obtained when the active material layer without the top electrode (directly after the annealing step) was exposed to air. A PCE increase of 88% compared to reference cells was the result, while it was just 30% with exposure after the electrode application. The parameters are listed in table 5.

TABLE 5: Average improvement by exposure to air before electrode application of glass | ITO | PEDOT:PSS | PCDTBT-CIS | Al solar cell.

	REFERENCE	IN AIR	
		just active material	whole device
V_{OC}	0.48 ± 0.00	0.51 ± 0.00 (+6%)	0.53 ± 0.00 (+11%)
J_{SC}	4.86 ± 0.01	6.21 ± 0.01 (+28%)	4.65 ± 0.15 (-4%)
FF	38.1 ± 0.34	53.3 ± 0.84 (+40%)	46.7 ± 0.86 (+22%)
PCE	0.89 ± 0.01	1.68 ± 0.03 (+88%)	1.16 ± 0.06 (+30%)

$n = 6$, each. All 70 vol% CIS, spin coated.

As an illustration figure 24 shows J-V characteristics of two solar cells with absorber layers fabricated from the same solution and similar preparation steps. One solar cell is untreated the other is treated with air (red and blue lines, respectively). From this figure and table 5 it can be seen that the FF improved the most, reaching values beyond 55%.

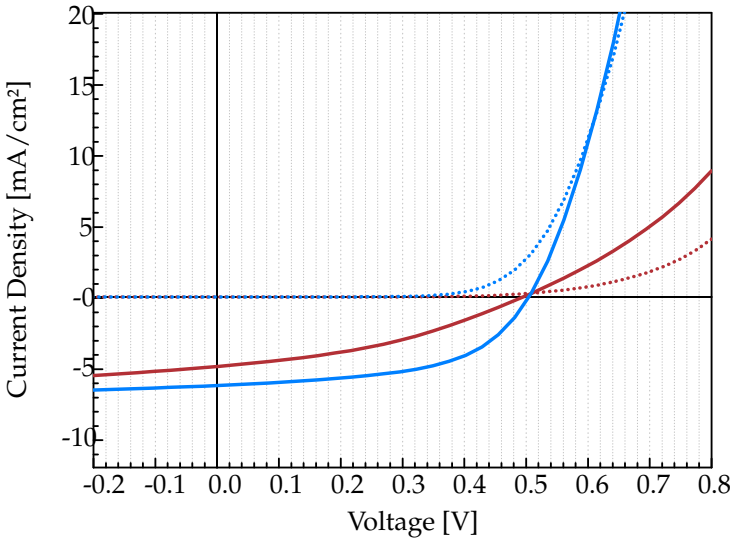

FIGURE 24: J-V curves: comparison of PCDTBT-CIS devices made from the same solution by spin coating without (red) and with (blue) oxygen treatment.

Oxygen is often discussed for its negative influence on solar cells. In context with polymers mostly for polymer degradation or for surface passivation of for instance inorganic silicon cells. Schafferhans et al. [37] investigated the influence of oxygen (from synthetic air) on P3HT-PCBM. They found that the exposure of these devices to synthetic air in the dark resulted in a loss of J_{SC} of 60% within 120 hours, in illumination all cell parameters decreased. Oxygen degradation under illumination decreased the PCE by 30% within 3 hours. On the contrary Schafferhans et al. [37] observed an increased charge-carrier concentration by CELIV measurements which can be contributed to oxygen doping known for P3HT.

Besides polymer doping, aluminum electrode oxidation has been suggested [2, 19, 39] to increase the V_{OC}, and therefore the PCE. Bernède et al. [2] exposed organic solar cells with aluminum to air. They attributed the observed high V_{OC} to the formation of an ultra-thin Al_2O_3-layer at the polymer-electrode interface. An effect also which was found by Singh et al. [39, 40].

An aluminum oxide layer could have been formed in devices with an aluminum electrode. However, when silver was used as the electrode material improvements were observed too.

Glass | ITO | PEDOT:PSS | PCDTBT/CIS | Ag solar cells, without air treatment, showed already a high J_{SC} (up to 11 mA/cm²). The treatment with air in this case improved the FF, as well as the V_{OC}. This suggests the air treatment improvements are caused by more than just the formation of a interfacial layer. From observations in this work two things are suggested: An Al_2O_3 layer does not really influence the performance of PCDTBT/CIS cells, or the thickness of this layer quickly exceeds the critical value and leads to dominating disadvantages (like degradation processes), as was suggested by Dunst [8].

To determine the role of oxygen for performance enhancement, active layers were further treated with synthetic air: 20.5 vol% oxygen, $<$ 5 vpm water vapor, $<$ 0.1 vpm CH_4, $<$ 0.5 vpm CO_2, $<$ 0.1 vpm NOx, rest: nitrogen. Only the active material layer was exposed to the synthetic air. This was similar to the experiments that led to the best results with air treatment. Under nitrogen atmosphere the substrates were placed in an air tight container. Then this container was flushed with synthetic air for 5 minutes. The synthetic air was removed by flushing with nitrogen and the devices were finished by evaporating the electrodes, again under nitrogen atmosphere. Interestingly, the treated solar cells showed no significant enhancement compared to reference cells without oxygen treatment. Therefore, it can be suggested that oxygen alone does not enhance the solar cell performance. Other contents of air such as water vapor might cause enhancements instead. This would have required additional experiments, which unfortunately could not be done due to time constraints.

Nevertheless, the highest V_{OC} in this study (614 mV) was measured for a glass | PEDOT:PSS | PCDTBT/CIS | Al device after exposing it to air for 5 minutes (see figure 25). Further the second best PCE of this study with 2.36% and a high FF of 58% was measured for an air treated device (70 vol% CIS). EQE data is shown in figure 26 and shows high resemblance to the UV-VIS spectra (figures on page 31). The active material converts light

to a major part at lower wavelengths, with an absolute maximum at 400 nm and a local maximum at 575 nm.

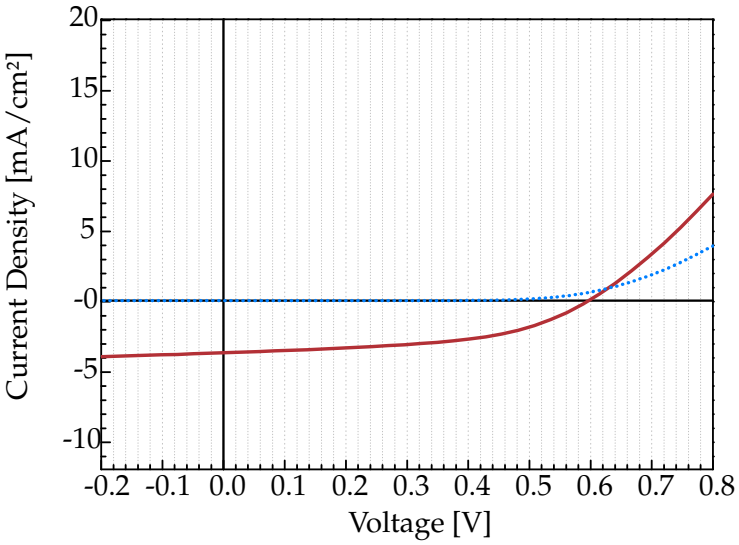

FIGURE 25: A solar cell treated with air for 5 minutes after the CIS annealing step showing a V_{OC} of 614 mV.

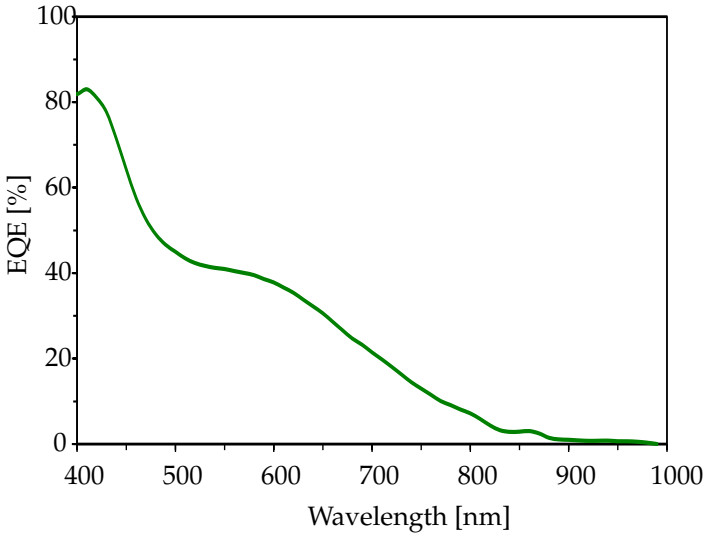

FIGURE 26: The EQE spectrum of a device with 2.36% PCE, treated with air.

Hybrid solar cells still can not keep up with organic solar cells in terms of efficiency. In these devices electron acceptors such as fullerene derivatives are used. One famous derivative is PCBM. A major difference between PCBM and nanoparticles is the rather simple surface structure of PCBM [49]. Additives that enhance the PCE of hybrid solar cells by modifying the microstructure of the nanoparticles or the interface between the nanoparticles and the polymer would be very elegant.

Fu et al. [12] studied the effect of molecular dipoles on the conjugated polymer-nanoparticle interface. They investigated these dipoles for ligand exchange and found efficiencies up to 4% using benzenethiol derivatives. The use of short chain alkylthiols or aromatic thiols as ligands helps to achieve high PCEs. Liu et al. [24] report a PCE of 5.5% and a FF of 67% for a low band-gap polymer and PbS_xSe_{1-x} alloy nanocrystals and attribute these good results (besides the high performance materials and the polymer-nanocrystal ratio) to the morphology. Zhou et al. [50] treated hybrid devices with an ethanedithiol-containing acetonitrile solution and observed enhancements in efficiency of 30% to 90%. An improvement of the charge separation at the donor-acceptor interface of hybrid solar cells with benzene-1,3-dithiol (BDT) treatment was shown by Chen et al. [4].

In this thesis the effect of BDT on PCDTBT-CIS cells was studied. Different methods (*i-iv*) were used to introduce the molecule into the layer.

At first BDT was dissolved in acetonitrile to produce a 0.01 M solution. This solution was dropped on the still wet polymer-xanthate layer (*i*), with the prospect to introduce the BDT molecules deeply into the layer. Unfortunately, but not surprisingly, the layer was destroyed by this treatment (see images in figure 27). Changing the solvent to isopropyl alcohol did not change the result.

The same solutions were dropped on the heat treated (dry) polymer-CIS layer (*ii*) for different durations (15 s, 30s, and 60 s) before excess solution was spinned off. In a first experiment this was performed together with

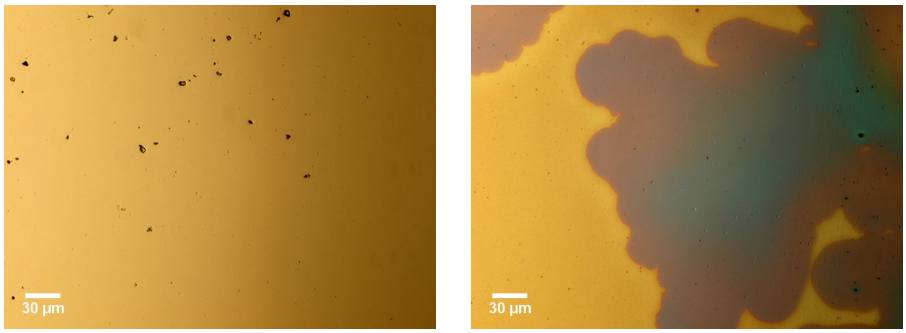

(A) Untreated surface, 400x. (B) Destructed surface, 400x.

FIGURE 27: Comparison of a untreated PCDTBT-CIS (70 vol%) layer to a destroyed one by drop coating. The drop coating was done before the tempering process. Afterwards both samples were tempered and electrodes were applied. (A) shows a normal surface in 400-fold magnification. In (B) the dark region where the drop first hit the surface is shown (400-fold magnification).

two kinds of reference cells. One kind of reference solar cells was not treated specially at all (reference *A*), while the other kind was treated with acetonitrile (reference *B*) to see effects of the solvent itself. The BDT-treatment resulted in an increase of all solar cell parameters in comparison to the reference cells. They further increased with longer treatment duration. Figure 28 shows the enhancement visually, the corresponding data can be found in table 6.

TABLE 6: Device parameters of solar cells treated with BDT compared to reference cells *A* and *B*. Experiment 1.

	A	*B*	15 s	30 s	60 s
V_{OC} average	0.36 ± 0.05	0.35 ± 0.06	0.40 ± 0.05	0.45 ± 0.03	0.45 ± 0.08
V_{OC} max.	0.41	0.40	0.46	0.48	0.51
J_{SC} average	2.81 ± 0.3	2.76 ± 0.3	3.22 ± 0.3	3.34 ± 0.3	3.41 ± 0.4
J_{SC} max.	3.21	3.20	3.43	3.59	3.81
FF average	32.3 ± 1.6	31.7 ± 1.5	38.6 ± 2.3	42.4 ± 2.2	43.2 ± 5.4
FF max.	34.1	33.4	41.2	45.5	47.7
PCE average	0.33 ± 0.09	0.32 ± 0.09	0.50 ± 0.11	0.64 ±0.11	0.68 ± 0.23
PCE max.	0.45	0.42	0.64	0.76	0.92

A second experiment was performed, additionally, with BDT dissolved in isopropyl alcohol and a treatment duration of 1.5 minutes. It showed again an enhancement by BDT treatment, however the acetonitrile solution seemed to enhance the influence of the BDT on the device performance

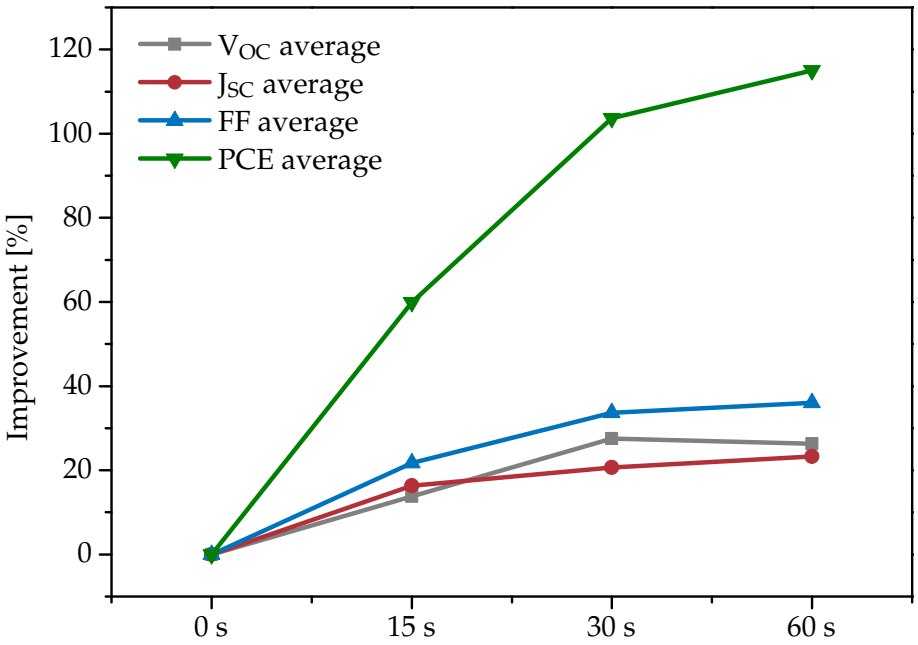

FIGURE 28: Improvement of PCDTBT-CIS cells by treatment (0 s, 15 s, 30 s, and 60 s) with benzene-1,3-dithiol 0.01 M in acetonitrile. Experiment 1.

more strongly. Observed was an average increase from the reference cells' PCE of 0.8% to 1.37% with BDT in acetonitrile, and from 0.8% to 1.14% with BDT in isopropyl alcohol. The solar cell parameters are listed in table 7.

TABLE 7: Device parameters of solar cells treated with BDT in different solvents for 1.5 minutes, compared to reference cells. Experiment 2.

	REFERENCE	ISOPROPYL ALK.	ACETONITRILE
V_{OC} average	0.46 ± 0.02	0.48 ± 0.04	0.52 ± 0.03
V_{OC} max.	0.48	0.51	0.53
J_{SC} average	4.65 ± 0.31	5.28 ± 0.64	5.73 ± 0.19
J_{SC} max.	4.87	6.01	5.88
FF average	37.1 ± 1.3	43.4 ±5.4	46.1 ± 5.2
FF max.	38.5	49.1	50.6
PCE average	0.80 ± 0.11	1.14 ± 0.33	1.37 ± 0.22
PCE max.	0.90	1.50	1.59

In comparison to the dropping method (*ii*), other performed methods, did not show satisfying positive effects on the resulting cells. Nevertheless, they are listed in the following paragraph.

It was observed that solutions with acetonitrile and isopropyl alcohol spread very easily and evenly on the substrate. To transfer this property to the solution with the polymer and the CIS precursors the BDT in the mentioned solvents (0.01 M) was added (*iii*). This could eventually improve the substrate coating and also introduce BDT into the active layer. However, PCDTBT is not soluble in acetonitrile and isopropyl alcohol (one reason why these solvents were chosen for the dropping method). Unfortunately already small amount of these solvents caused the polymer to precipitate, so that the resulting solar cells did not work efficiently.

To investigate the influence of BDT within the solution, 2 wt% BDT based on the solvent weight was directly added (*iv*). In comparison to reference cells the effect was too little to make a statement.

Additionally pyridine and 1,8-diiodooctane (DIO) were tested for additives with the same methods as BDT. Pyridine, a small molecule, has good chances to diffuse into the PCDTBT/CIS layer, and can coordinate to the nanoparticle surface. DIO, on the other hand, is known for enhancing the PCE of BHJ polymer solar cells. It is suggested that DIO allowed the PCBM to reorganize, resulting in better segregated nanophase structure and appropriate domain size [20, 32]. A possible similar effect with inorganic CIS nanoparticles should be investigated.

Similar to (*ii*) with BDT a 0.01 M pyridine acetonitrile solution was dropped onto the polymer-CIS layer for 1.5 minutes. The average PCE was $0.95 \pm 0.16\%$, which was a slight enhancement compared to the reference cells with 0.80 ± 0.11 % PCE. A repetition of this experiment did not deliver new insights. Because of the simple procedure, method (*ii*) was performed with a 0.01 M DIO acetonitrile solution. Compared to the reference cells, the result showed almost the same PCE (0.84 ± 0.30 % to 0.80 ± 0.11 % PCE, respectively).

According to literature, DIO is helping to organize the solar cell morphology when added to the solution [20, 32]. Therefore, 2 wt% based on the solvent was added to the solution as it was done in (*iv*). Also here

the treated solar cells showed no significant enhancement compared to reference cells without treatment.

5

OTHER POYLMER/CIS HYBRID SOLAR CELLS

5.1 PFFBT4T-2OD/CIS HYBRID SOLAR CELLS

In 2014, Liu et al. [23] investigated the morphology and aggregation of organic solar cells. Among the three donor polymers they investigated was the very promising polymer PffBT4T-2OD: poly[(5,6-difluoro-2,1,3-benzothiadiazol-4,7-diyl)-alt-(3,3‴-di(2-octyldodecyl)-2,2′;5′,2″;5″,2‴-quaterthiophen-5,5‴-diyl)].
The structure is shown below (figure 29), the full name can be found in section 8.1. The polymer shows high charge-carrier mobility ($1.5 - 3.0 * 10^{-2}$ $cm^2/V * s$). An optimized morphology with "highly crystalline, sufficiently pure, yet reasonably small polymer domains" [23] allowed the realization of very high efficiencies and FF in combination with fullerene derivative acceptors. With a comparably high film thicknesses of 300 nm solar cells with PffBT4T-2OD are candidates for cost-efficient roll-to-roll production methods. The combination of PffBT4T-2OD and $PC_{71}BM$ resulted in solar cells with a very high PCE over 10% [23]. Thus, this polymer is also called *PCE11*.

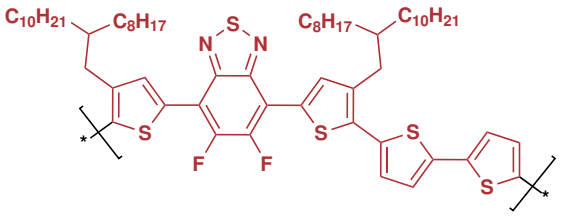

FIGURE 29: The structure of the conjugated polymer PffBT4T-2OD (also PCE-11).

In this work the combination of PffBT4T-2OD and CIS nanoparticles for solar cell absorber layer material was investigated. Two experiments were performed with PffBT4T-2OD and CIS (*i, iii*), one was performed

with $PC_{61}BM$ as a control experiment (*ii*). While the combination of PffBT4T-2OD and CIS resulted in very low PCEs, the control experiment with $PC_{61}BM$ showed an average PCE of almost 5%. Important experimental settings and the solar cell parameters are shown in table 8. The experiments are further described in the following paragraph.

TABLE 8: Experimental settings and solar cell parameters with PffBT4T-2OD.

	i	*ii*	*iii*
EXP. SETTINGS			
Polymer Conc. [mg/ml]	5	9	9
Temperature* [°C]	110	110	110
Acceptor	CIS	$PC_{61}BM$	CIS
CIS Loading [%]	70	–	71
Polymer-PCBM ratio	–	1:2.5	–
Speed [rpm]	1400	800	1200
PARAMETERS			
Layer Thickness [nm]	130 ± 6.5	248 ± 26	168 ± 10
V_{OC}	0.06 ± 0.04	0.73 ± 0.01	0.11 ± 0.02
J_{SC}	0.90 ± 0.57	11.35 ± 0.20	0.24 ± 0.03
FF	19.3 ± 5.1	59.5 ± 2.9	24.7 ± 2.6
PCE	0.02 ± 0.02	4.89 ± 0.27	0.007 ± 0.001

* Fabrication temperature: in a next step the CIS nanoparticles formation was performed by heat treatment up to temperatures of 195 °C.

The experiments were based on the procedure described by Liu et al. and on earlier performed experiments with PCDTBT/CIS solar cells. (*i*) 5 mg/ml PffBT4T-2OD was mixed in CB/DCB 1+1 and the metal xanthate precursors for 70 vol% CIS were added. The mixture was very viscous. When heated up to temperatures above 80 °C it became less viscous and the color of the polymer changed from a dark green to a strong berry-red. A sign of completed polymer dilution. The layer was applied by spin coating with the solution and the substrates heated to 110 °C (to keep the PffBT4T-2OD dissolved while coating). The solar cells from this experiment showed very low values for V_{OC}, J_{SC}, and FF, resulting in a very low PCE. The experiment was repeated with the same settings, however, again it showed almost the same results. The film thickness was about 130 nm.

(*ii*) Liu et al. used a higher concentration of 9 mg/ml and described the polymer-PCBM mixture as gel-like when at room temperature. A solution was produced with the same concentration and $PC_{61}BM$ with a 1:2.5 polymer-fullerene weight ratio. The applied layers had 248 nm on average and a very rough surface (73 $\pm$ 7 nm). Nevertheless, an average PCE of 4.89% (maximum 5.24%) was achieved without any further optimization necessary.

To obtain thicker layers than in (*i*), the same 9 mg/ml PffBT4T solution was used and mixed with CIS precursors. A rotation speed in the range of 800 to 1000 rpm and this solution produced too thick layers ($>$ 1000 nm). Therefore, a higher spinning rate was used for the next experiments (iii). The solar cells with a 168 nm layer were observed to be even less efficient than (*i*).

5.2 PPDTBT/CIS HYBRID SOLAR CELLS

Poly[4,8-bis(5-(2-ethylhexyl)thiophen-2-yl)benzo[1,2-b:4,5-b′] dithiophene-2,6-diyl-1,4-bis(5-bromothiophen-2-yl)-6-(2-decyltetradecyl)-5H-pyrrolo[3,4-d]pyridazine-5,7(6H)-dione-5,5″-diyl] abbreviated PPDTBT is a relatively new polymer, showing suitable properties for utilization in solar cells: A conjugated π-system, wide absorption, and a low LUMO level. Zhang et al. [48] reported organic solar cells with efficiencies over 3.5%. Its structure is shown in figure 30 below.

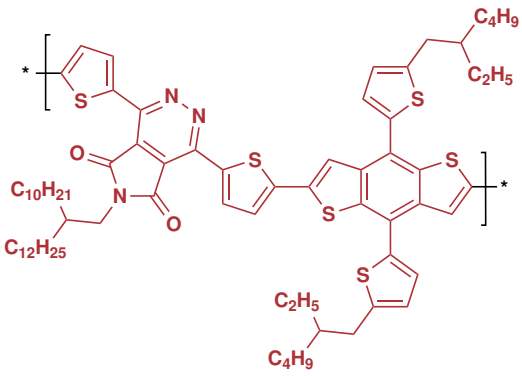

FIGURE 30: The structure of the conjugated polymer PPDTBT.

Devices with an active material containing 70 vol% CIS achieved PCEs above 1%. Special attention was payed on the production of smooth, big-particle-free layers. Therefore, the solution was filtered before applying it on the substrate. A layer thickness of 120 to 130 nm seemed to be favorable. This is thicker than for PCDTBT solar cells. The average values for the devices with the best PCE are shown in table 9.

TABLE 9: Parameters of the best five PPDTBT cells.

V_{OC}	J_{SC}	FF	PCE
[V]	[mA/cm²]	[%]	[%]
0.44 ± 0.05	6.88 ± 0.34	47.0 ± 4.80	1.67 ± 0.09

The best devices had a thickness of approximately 126 nm, leading to a maximum PCE of 1.77%. The J-V characteristics and the EQE data of this device is shown in figure 31 and 32, respectively.

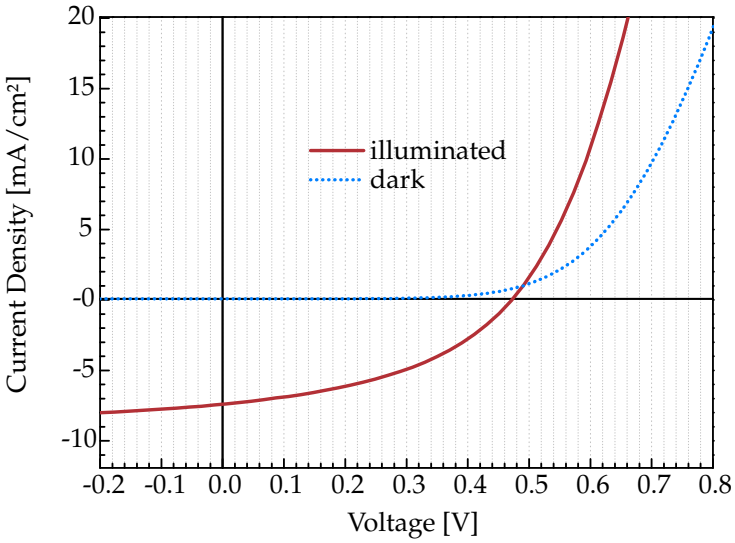

FIGURE 31: The J-V characteristics of a device with PPDTBT and 1.77% PCE.

An absorption spectrum of PPDTBT found in literature had an absolute maximum at approximately 560 nm (in a broad range of 300 nm to 400 nm) and a second local maximum at 350 nm [48]. Compared to this spectrum, the EQE curve shows the same maximum but a different shape. With a smaller calculated band gap than PCDTBT the calculated J_{SC} was higher. However, the observed values of the investigated devices were in the same range.

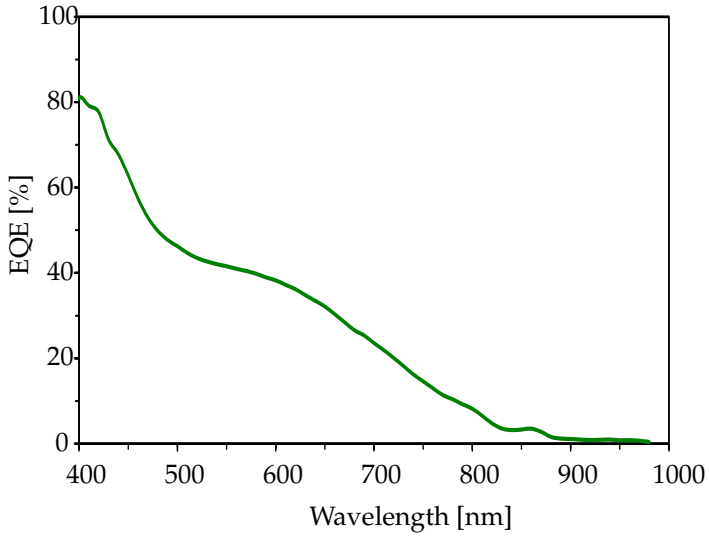

FIGURE 32: The EQE of a device with PPDTBT and 1.77% PCE.

The achieved PCEs with the polymers PPDTBT and PffBT4T-2OD were lower than those of PCDTBT/CIS devices. However, many more attempts and experiments to enhance the PCE were performed with PCDTBT.

6

CONCLUSION

The in-situ approach to fabricate absorber layers for polymer/CIS hybrid solar cells proved itself as a facile and elegant method. The nanoparticles were formed directly within the polymer matrix from copper and indium xanthate precursors via heat treatment below 200 °C. Influences of different fabrication parameters or organic molecules on the solar cells were tested. Varying the polymer/nanoparticle weight ratio, changing the polymer phase or introducing organic compounds into the layer are some examples. The polymer/CIS hybrid solar cells seemed to be very sensitive towards their environment during fabrication. Therefore, a great attention was payed on finding a reproducible system.

UV-Vis absorption spectroscopy showed a higher absorption with higher CIS loading in the layer. Solar cells with 70 vol% CIS in the active material showed a V_{OC} of 0.48 V, a J_{SC} of 8.01 mA/cm², a very high FF of 59.2 % and a high average PCE of 2.24%. A layer thickness of 70 to 90 nm was found to be optimal for cells with low Mw PCDTBT. Additionally, a higher Mw PCDTBT was used. This should change the active material morphology to achieve higher PCEs. Nonetheless, no real enhancement was observed by increasing the molecular weight alone.

The higher Mw was less soluble in the primarily used chlorobenzene and dichlorobenzene had to be used in a solvent mixture. The polymer had to be dissolved at elevated temperatures. This caused challenging issues for smooth surfaces as the polymer tended to precipitate in little particles in the applied active material layer. The thickness of the PCDTBT/CIS layer in the devices was stronger and led to the best results when it was approximately 100 nm thick. Here, on average, a V_{OC} of 0.54 V, a J_{SC} of 9.94 mA/cm², a FF of a 39.1% and a PCE of 2.08% were achieved. Compared to the low Mw a 20% lower FF decreased the efficiency even though the V_{OC} and J_{SC}

were higher. A thinner layer of 78 nm (close to the 74 nm of the low Mw polymer) decreased the cell parameters further and a lower PCE of 1.69% was measured.

A significant enhancement was found when the active material was exposed to air. A 5-minute-exposure improved the PCE by 80% in average compared to reference cells. When the whole device was exposed an enhancement of only 30% was observed. The exposure to synthetic air with a very low amount of water vapor (below 0.5 vpm), however, showed no significant improvement compared to reference cells.

Mainly, aluminum and silver were used as metal electrode materials. Due to their different work functions, solar cells with aluminum electrodes led to higher V_{OC} values. However, silver showed a more predictable behaviour during the evaporation process and made this process well reproducible. Besides these advantages, J_{SC} values higher than 7 mA/cm² were achieved regularly. The best solar cell in this work was built with a silver electrode. The device revealed a PCE of 2.45% and its J-V curve under illumination is shown below in figure 33.

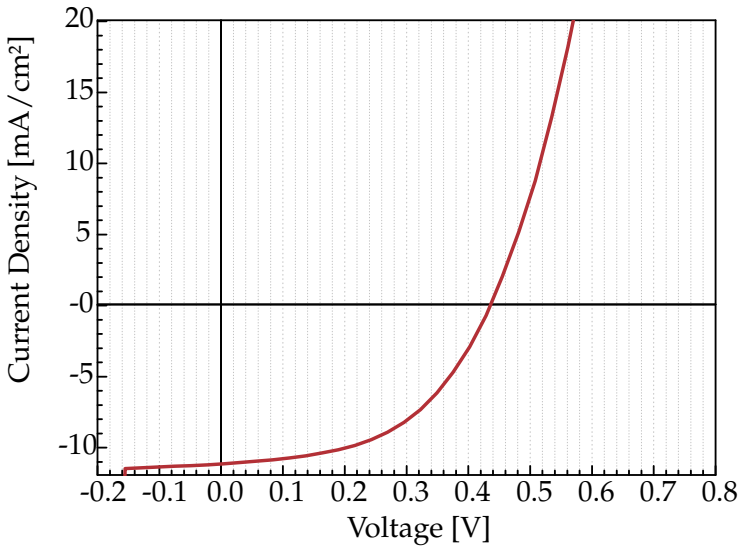

FIGURE 33: Illuminated J-V curve of a device with Ag-electrode and 2.45% PCE.

The influence of additives was also tested. Benzene-1,3-dithiol (BDT) affected the cell performance when it was dropped in a 0.01 M acetonitrile solution onto the tempered PCDTBT/CIS layer. In comparison to reference

cells with a PCE of 0.90% a PCE of 1.59% was achieved. On the other hand, the PCE was not enhanced by adding the BDT into the solution in various ways. Furthermore, pyridine and 1,8-diiodooctane were used in similar treatments, but no solar cell with a high PCE was produced.

Although, PffBT4T-2OD seemed to be promising because very high PCEs were measured in polymer/PCBM solar cells, no well performing polymer/CIS solar cell could be realized with it. With PffBT4T it was not possible to produce smooth layers with an appropriate thickness. For PffBT4T/PCBM solar cells, layer thicknesses of around 200 nm are preferable. The application of the polymer/metal xanthate film produced either reasonably smooth surfaces but too thin layers, or thicker layers with very rough surfaces.

PPDTBT turned out to behave similarly to PCDTBT. Filtered solution produced smooth surfaces. With a PPDTBT/CIS layer thickness of 120 nm to 130 nm the best results were found. The highest achieved PCE was 1.77%, which is in the range of PCDTBT/CIS devices. Compared to the the best PCDTBT/CIS devices the J_{SC}, as well as the FF were lower: 11 mA/cm² and 58% for PCDTBT, and 7.5 mA/cm² and 43% for PPDTBT. Nonetheless, an increase of the PCE of PPDTBT/CIS devices beyond 2% can be possible with further treatments.

Polymer/CIS hybrid devices with an absorber layer produced via the in-situ route can be produced quickly and efficiently. This shows that they are very well suitable for roll-to-roll processes. The many possibilities to enhance their efficiency are too vast for the constrained duration of a master thesis. Nevertheless, it was shown that certain features (such as a CIS content of 70 vol%) promise the best efficiency and further, simple treatments (e.g. with air or BDT-solution) can increase the efficiency. The system was adoptable to two different conjugated polymers (PCDTBT and PPDTBT), and eventually could be adoptable to many more.

As already mentioned, there are ways to enhance the devices further. Additional investigations on the influence of other additives and the ways to introduce them into the absorber layer, as well as the influence of air can

be very useful. Regarding air the influence of water should be investigated further. Ideally a combination of positive effects could lead to PCEs higher 3%.

Part III

EXPERIMENTAL

7

DEVICE FABRICATION

SUBSTRATE PREPARATION: The glass substrates had dimensions of either 75 x 24 mm (for doctor plating) or 15 x 15 mm (for spin coating). All substrates were already partly coated with indium tin oxide (ITO). Visible dust particles were removed and the substrates were further cleaned in isopropyl alcohol in an ultra sound bath. Before inter-facial layers or active materials were applied the alcohol was removed in a nitrogen stream and the substrates were etched in an oxygen plasma to activate the surface.

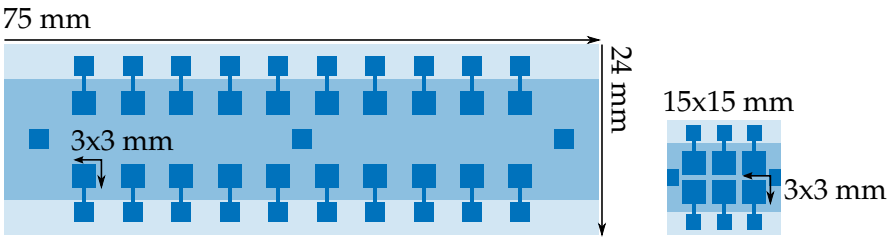

FIGURE 34: Solar cell schemes. ITO-substrate, coated active material and metal electrodes. A 20 cell substrate for doctor blading (left) and a 6 cell subtrate for spi coating (right).

PEDOT:PSS LAYER: An inferfacial layer of PEDOT:PSS was applied from aqueous solution (Heraeus Clevios™ 4083) by spin coating at 2500 rpm for 30 s. The residual water was removed on a hot plate at 150 °C for 15 minutes in nitrogen atmosphere.

ACTIVE LAYER CASTING: All active layer casting steps were done in a glovebox under nitrogen atmosphere.

DOCTOR BLADING: The hot plate was set to the preferred temperature and the blade height and speed was adjusted. If not mentioned

otherwise blade height and speed was 100 nm and 7.5 mm/s, respectively. 30 μl of active material solution was added and the coating started.

SPIN COATING: For spin coating rotation speed, acceleration and duration was set. If necessary the substrates and the solutions have been heated. If not mentioned differently elsewhere 30 μl solution were added evenly and the program started immediately.

CIS FORMATION STEP: After applying the active layer from a polymer-xanthate solution the substrates and the active layer were heated up to a temperature of 195 °C for 15 minutes and kept at this temperature for another 15 minutes to produce the CIS nanoparticles.

ELECTRODE EVAPORATION: The substrates were placed into an evaporation mask inside an evaporation chamber. The metal was applied from vapor at reduced pressure (10^{-5} mbar) in nitrogen atmosphere.

TITANIUM OXIDE INTERMEDIATE LAYER: The substrates were placed in the evaporation chamber under air. The chamber was evaporated and a piece of titanium wire thermally evaporated onto the substrates.

DROP TREATMENT FOR THE INVESTIGATION OF ADDITIVES: The layers were prepared as needed. Then the substrate was put on the spin coater and 50 µl of the additive solution was dropped onto the layer and the was timer started. After the specified time the spin coater started to accelerate with 1000 rpm/s to 4000 rpm and was at this speed for 10 s to remove the excess of solution. Then the surfase was washed with pure solvent and the same spin coating program, followed of a 5 minute drying step.

8

MATERIALS AND EQUIPMENT

8.1 POLYMERS

The conjugated polymers used in this work are listed below with their acronym and full name.

Polymeres used for Devices

PCDTBT:	poly[N-9′-heptadecanyl-2,7-carbazole-alt-5,5-(4,7-di-2-thienyl-2′,1′,3′-benzothiadiazole)]
PffBT4T-2OD:	poly[(5,6-difluoro-2,1,3-benzothiadiazol-4,7-diyl)-alt-(3,3‴-di(2-octyldodecyl)-2,2′;5′,2″;5″,2‴-quaterthiophen-5,5‴-diyl)]
PPDTBT:	Poly[4,8-bis(5-(2-ethylhexyl)thiophen-2-yl)benzo[1,2-b:4,5-b′]dithiophene-2,6-diyl-1,4-bis(5-bromothiophen-2-yl)-6-(2-decyltetradecyl)-5H-pyrrolo[3,4-d]pyridazine-5,7(6H)-dione-5,5″-diyl]

Mentioned Polymers

PSiFDBT:	Poly[2,7-(9,9-dioctyl-dibenzosilole)-alt-4,7-bis(thiophen-2-yl)benzo-2,1,3-thiadiazole]
P3HT:	Poly(3-hexylthiophen-2,5-diyl)

Purchased and used chemicals and materials are listed below in table 10. Materials that were synthesized at the Graz University of Technology are listed in table 11.

TABLE 10: List of purchased chemicals and materials.

	PURCHASED FROM
PCDTBT, low Mw	1-Material
PCDTBT, high Mw	1-Material
PffBT4T-2OD (PCE11)	1-Material
Acetonitrile 99.8%	Sigma Aldrich
Benzene-1,3-dithiol 99%	Sigma Aldrich
Chlorobenzene 99.9%	Sigma Aldrich
Dichlorobenzene 99%	Sigma Aldrich
1,8-Diiodooctane 97%	Sigma Aldrich
Isopropyl alcohol 99.8%	Sigma Aldrich
$PC_{61}BM$	Solenne
Pyridine 99%	Sigma Aldrich
Synthetic air 5.0	Messer Austria GmbH

TABLE 11: List of materials synthesized at the Graz University of Technology.

	SYNTHESIS
PPDTBT	Synthesized by Dipl- Ing. Dr.tech. Astrid Knall.
Cu- and In-xanthates	The metal xanthates (copper O-2,2-dimethylpentan-3-yl dithiocarbonate, indium O-2,2-dimethylpentan-3-yl dithiocarbonate) were synthesized by Aglycon Dr. Spreitz KG, Austria, based on a published protocol [34] and afterwards recrystallized from chloroform/methanol.

8.3 USED EQUIPMENT

Equipment used in this work to produce or characterize the solar cells are listed in table 12.

TABLE 12: List of used equipment.

DEVICE	APPLICATION
Braun Glovebox	Glovebox with evaporation chamber.
Bruker *DektakXT*	Profilometer.
Diener electronics *Femto*	Surface plasma treatment.
Fraunhofer ISE *WPVS* reference cell	Adjust the light source to 100 mW/cm^2 for the J-V measurements.
Inficon *SQM-160*	Rate and thickness monitor for vacuum evaporation processes.
Keithley *SourceMeter 4ZA4, 2400 series line*	I-V characterization of the solar cells.
Laurell technologies *Spincoater model WS-65MMZ-23NPPB*	Coating substrates with active material
SPI *Spin-Coater KW-4A*	Coating glass/ITO substrates with PEDOT:PSS.
VWR *Ultrasonic Cleaner*	

LIST OF FIGURES

LIST OF TABLES

ACRONYMS

AM air mass

BHJ bulk heterojunction

BDT benzene-1,3-dithiol

CB chlorobenzene

CELIV charge carrier extraction by linearly increasing voltage

CIS copper indium disulfide

DCB dichlorobenzene

DIO 1,8-diiodooctane

DNI direct normal irradiation

EQE external quantum efficiency

FF fill factor

GHI global horizontal irradiation

HOMO highest occupied molecular orbital

ITO indium tin oxide

IQE internal quantum efficiency

J_{SC} short circuit current density

LUMO lowest unoccupied molecular orbital

Mw molecular weight

P3HT poly(3-hexylthiophen-2,5-diyl)

PCBM [6,6]-phenyl-C_{61}butyric acid methyl ester

PCDTBT A conjugated polymer. See section 8.1

PCE power conversion efficiency

PEDOT:PSS poly-3,4-ethylendioxythiophene/polystyrolsulfonate

PffBT4T-2OD A conjugated polymer. See section 8.1

PV photovoltaic

QE quantum efficiency

SAED selected area electron diffraction

TEM transmission electron microscopy

UV-VIS ultraviolet and visible light

V_{OC} open circuit voltage

BIBLIOGRAPHY

[1] Mario Arar, Manfred Gruber, Michael Edler, Wernfried Haas, Ferdinand Hofer, Neha Bansal, Luke X Reynolds, Saif a Haque, Karin Zojer, Gregor Trimmel, and Thomas Rath. "Influence of morphology and polymer:nanoparticle ratio on device performance of hybrid solar cells-an approach in experiment and simulation. SI." In: *Nanotechnology* 24.48 (2013), p. 484005. URL: http://www.ncbi.nlm.nih.gov/pubmed/24196417 (cit. on pp. 17, 19, 20, 23, 24).

[2] J. C. Bernède, A. Godoy, L. Cattin, F. R. Diaz, M. Morsli, and M. A. DelValle. *Organic Solar Cells Performances Improvement Induced by Interface Buffer Layers*. February. 2010, pp. 223–266. URL: http://www.intechopen.com/books/solar-energy (cit. on p. 37).

[3] Weiran Cao et al. "Recent progress in organic photovoltaics: device architecture and optical design." In: *Energy & Environmental Science* 7.7 (2014), p. 2123. URL: http://xlink.rsc.org/?DOI=c4ee00260a (cit. on p. 7).

[4] Hsieh Chih Chen, Chih Wei Lai, I. Che Wu, Hsin Ru Pan, I. Wen P Chen, Yung Kang Peng, Chien Liang Liu, Chun-Hsien Chen, and Pi Tai Chou. "Enhanced performance and air stability of 3.2% hybrid solar cells: How the functional polymer and cdte nanostructure boost the solar cell efficiency." In: *Advanced Materials* 23.45 (2011), pp. 5451–5455 (cit. on pp. 15, 40).

[5] Rosaria Ciriminna, Francesco Meneguzzo, Mario Pecoraino, and Mario Pagliaro. "Rethinking solar energy education on the dawn of the solar economy." In: *Renewable and Sustainable Energy Reviews* 63 (2016), pp. 13–18. URL: http://linkinghub.elsevier.com/retrieve/pii/S1364032116301186 (cit. on pp. 2, 3).

[6] Kevin M. Coakley and Michael D. McGehee. "Conjugated polymer photovoltaic cells." In: *Chemistry of Materials* 16.23 (2004), pp. 4533–4542. URL: justcite (cit. on p. 27).

[7] Seth B. Darling and Fengqi You. "The case for organic photovoltaics." In: *RSC Adv.* 3 (2013), pp. 17633–17648 (cit. on p. 8).

[8] Sebastian Dunst. "Polymer – copper indium sulphide hybrid solar cells: Operational stability and novel device architectures." PhD thesis. TU Graz, 2016, p. 172 (cit. on pp. 17, 20, 23, 38).

[9] Sebastian Dunst, Thomas Rath, Stefan Moscher, Lukas Troi, Matthias Edler, Thomas Griesser, and Gregor Trimmel. "Influence of TiOx and Ti cathode interlayers on the performance and stability of hybrid solar cells." In: *Solar Energy Materials and Solar Cells* 130 (2014), pp. 217–224 (cit. on pp. 9, 35).

[10] Christopher Fradler, Thomas Rath, Sebastian Dunst, Ilse Letofsky-Papst, Robert Saf, Birgit Kunert, Ferdinand Hofer, Roland Resel, and Gregor Trimmel. "Flexible polymer/copper indium sulfide hybrid solar cells and modules based on the metal xanthate route and low temperature annealing." In: *Solar Energy Materials and Solar Cells* 124 (2014), pp. 117–125. URL: http://dx.doi.org/10.1016/j.solmat.2014.01.043 (cit. on pp. 17, 20, 23).

[11] Fraunhofer ISE. *Photovoltaics Report, updatet: 11 Mach 2016*. Tech. rep. 2016, p. 43 (cit. on p. 8).

[12] Weifei Fu, Ling Wang, Jun Ling, Hanying Li, Minmin Shi, Jiangeng Xue, and Hongzheng Chen. "Highly efficient hybrid solar cells with tunable dipole at the donor–acceptor interface." In: *Nanoscale* 6.18 (2014), p. 10545. URL: http://xlink.rsc.org/?DOI=C4NR02339K (cit. on pp. 9, 21, 40).

[13] Martin A. Green, Keith Emery, Yoshihiro Hishikawa, Wilhelm Warta, and Ewan D. Dunlop. "Solar cell efficiency tables (version 40)."

In: *Progress in Photovoltaics: Research and Applications* 20.5 (2012), pp. 606–614. arXiv: 1303.4604 (cit. on p. 15).

[14] Serap Günes, Helmut Neugebauer, and Niyazi Serdar Sariciftci. "Conjugated polymer-based organic solar cells." In: *Chemical Reviews* 107.4 (2007), pp. 1324–1338. arXiv: arXiv:1011.1669v3 (cit. on p. 27).

[15] Alan J. Heeger, Alan G. MacDiarmid, and Hideki Shirakawa. *Nobel Prize for the Discovery and Development of Conductive Polymers*. 2000 (cit. on p. 15).

[16] Sandra Hofer. "Synthesis and Characterisation of CuInS2 - Nanoparticles for Hybrid Solar Cells." PhD thesis. 2005 (cit. on p. 20).

[17] Harald Hoppe and N. Serdar Sariciftci. "Polymer solar cells." In: *Advances in Polymer Science*. Vol. 214. 1. Berlin, Heidelberg: Springer Berlin Heidelberg, 2008, pp. 1–86. URL: http://link.springer.com/10.1007/12{_}2007{_}121 (cit. on p. 27).

[18] Krischan F. Jeltsch, Martin Schädel, Jörg Bernd Bonekamp, Phenwisa Niyamakom, Frank Rauscher, Hans W. A. Lademann, Ines Dumsch, Sybille Allard, Ullrich Scherf, and Klaus Meerholz. "Efficiency enhanced hybrid solar cells using a blend of quantum dots and nanorods." In: *Advanced Functional Materials* 22.2 (2012), pp. 397–404. URL: http://doi.wiley.com/10.1002/adfm.201101809 (cit. on p. 15).

[19] N. Karst and J. C. Bernède. "On the improvement of the open circuit voltage of plastic solar cells by the presence of a thin aluminium oxide layer at the interface organic/aluminium." In: *Physica Status Solidi a-Applications and Materials Science* 203.10 (2006), R70–R72 (cit. on p. 37).

[20] Jae Kwan Lee, Wan Li Ma, Christoph J. Brabec, Jonathan Yuen, Ji Sun Moon, Jin Young Kim, Kwanghee Lee, Guillermo C. Bazan, and Alan J. Heeger. "Processing additives for improved efficiency from bulk heterojunction solar cells." In: *Journal of the American Chemical Society* 130.11 (2008), pp. 3619–23. arXiv: arXiv:1408.1149. URL: http://

pubs.acs.org/doi/abs/10.1021/ja710079whttp://dx.doi.org/10.1021/ja710079w (cit. on p. 43).

[21] H. J. Lewerenz. "Development of copperindiumdisulfide into a solar material." In: *Solar Energy Materials and Solar Cells* 83.4 (2004), pp. 395–407 (cit. on p. 19).

[22] Gang Li, Rui Zhu, and Yang Yang. "Polymer solar cells." In: *Nat. Photonics* 6.3 (2012), pp. 153–161. URL: http://www.nature.com/doifinder/10.1038/nphoton.2012.11 (cit. on p. 15).

[23] Yuhang Liu, Jingbo Zhao, Zhengke Li, Cheng Mu, Wei Ma, Huawei Hu, Kui Jiang, Haoran Lin, Harald Ade, and He Yan. "Aggregation and morphology control enables multiple cases of high-efficiency polymer solar cells." In: *Nature Communications* 5:5293.9 (2014), doi: 10.1038/ncomms6293. URL: http://dx.doi.org/10.1038/ncomms6293 (cit. on pp. 21, 27, 45–47).

[24] Zeke Liu, Yaxiang Sun, Jianyu Yuan, Huaixin Wei, Xiaodong Huang, Lu Han, Weiwei Wang, Haiqiao Wang, and Wanli Ma. "High-efficiency hybrid solar cells based on polymer/PbSx Se1-x nanocrystals benefiting from vertical phase segregation." In: *Advanced materials (Deerfield Beach, Fla.)* 25.40 (2013), pp. 5772–8. URL: http://doi.wiley.com/10.1002/adma.201302340http://www.ncbi.nlm.nih.gov/pubmed/23934968 (cit. on p. 40).

[25] Tom Markvart and Luis Castañer. *Principles of Solar Cell Operation*. Elsevier Ltd, 2012, pp. 7–31. arXiv: arXiv:1011.1669v3. URL: http://dx.doi.org/10.1016/B978-0-12-385934-1.00001-5 (cit. on pp. 8–10, 12).

[26] Gon Namkoong, Jaemin Kong, Matthew Samson, In-wook Hwang, and Kwanghee Lee. "Active layer thickness effect on the recombination process of PCDTBT:PC71BM organic solar cells." In: *Organic Electronics* 14.1 (2013), pp. 74–79. URL: http://dx.doi.org/10.1016/j.orgel.2012.10.025 (cit. on p. 27).

[27] Felix Nickel, Christian Sprau, Michael F. G. Klein, Panagiota Kapetana, Nico Christ, Xin Liu, Soenke Klinkhammer, Uli Lemmer, and Alexander Colsmann. "Spatial mapping of photocurrents in organic solar cells comprising wedge-shaped absorber layers for an efficient material screening." In: *Solar Energy Materials and Solar Cells* 104 (2012), pp. 18–22. URL: http://dx.doi.org/10.1016/j.solmat.2012.04.026 (cit. on p. 27).

[28] Stefan D. Oosterhout, Martijn M. Wienk, Svetlana S. VanBavel, Ralf Thiedmann, L. Jan Anton Koster, Jan Gilot, Joachim Loos, Volker Schmidt, and René A. J. Janssen. "The effect of three-dimensional morphology on the efficiency of hybrid polymer solar cells." In: *Nature materials* 8.10 (2009), pp. 818–824. URL: http://www.nature.com/doifinder/10.1038/nmat2533http://dx.doi.org/10.1038/nmat2533 (cit. on p. 15).

[29] PV Education. *Double Diode Model*. URL: http://www.pveducation.org/pvcdrom/characterisation/double-diode-model (visited on 06/10/2016) (cit. on p. 12).

[30] PV Education. *Quantum Efficiency*. URL: http://www.pveducation.org/pvcdrom/solar-cell-operation/quantum-efficiency (visited on 07/23/2016) (cit. on p. 14).

[31] PV Education. *Standard Solar Spectra*. URL: http://www.pveducation.org/pvcdrom/appendices/standard-solar-spectra (visited on 06/09/2016) (cit. on p. 4).

[32] Jeffrey Peet, Michelle L. Senatore, Alan J. Heeger, and Guillermo C. Bazan. "Bulk Heterojunction Solar Cells: The Role of Processing in the Fabrication and Optimization of Plastic Solar Cells." In: *Advanced Materials* 21.14-15 (2009), n/a–n/a. URL: http://doi.wiley.com/10.1002/adma.200990046http://dx.doi.org/10.1002/adma.200990046 (cit. on p. 43).

[33] Thomas Rath and Gregor Trimmel. "In situ syntheses of semiconducting nanoparticles in conjugated polymer matrices

and their application in photovoltaics." In: *Hybrid Materials* 1.1 (2014), pp. 15–36. URL: http://www.degruyter.com/view/j/hyma.2013.1.issue-1/hyma-2013-0003/hyma-2013-0003.xml (cit. on p. 15).

[34] Thomas Rath et al. "A direct route towards polymer/copper indium sulfide nanocomposite solar cells." In: *Advanced Energy Materials* 1.6 (2011), pp. 1046–1050 (cit. on pp. 9, 15, 17, 20, 58).

[35] Shenqiang Ren, Liang-Yi Chang, Sung-Keun Lim, Jing Zhao, Matthew Smith, Ni Zhao, Vladimir Bulović, Moungi Bawendi, and Silvija Gradecak. "Inorganic-organic hybrid solar cell: bridging quantum dots to conjugated polymer nanowires." In: *Nano letters* 11.9 (2011), pp. 3998–4002. URL: http://www.ncbi.nlm.nih.gov/pubmed/21859097 (cit. on p. 15).

[36] Edward H Sargent. "Colloidal quantum dot solar cells." In: *Nature Photonics* 6.March (2012), pp. 133–135 (cit. on p. 2).

[37] Julia Schafferhans, Andreas Baumann, Alexander Wagenpfahl, Carsten Deibel, and Vladimir Dyakonov. "Oxygen doping of P3HT:PCBM blends: Influence on trap states, charge carrier mobility and solar cell performance." In: *Organic Electronics: physics, materials, applications* 11.10 (2010), pp. 1693–1700. arXiv: 1008.4230 (cit. on p. 37).

[38] Sigma Aldrich. *PCDTBT*. URL: http://www.sigmaaldrich.com/catalog/product/aldrich/753998?lang=de{\&}region=AT (visited on 07/31/2016) (cit. on p. 27).

[39] V. P. Singh, R. S. Singh, B. Parthasarathy, A. Aguilera, J. Anthony, and M. Payne. "Copper-phthalocyanine-based organic solar cells with high open-circuit voltage." In: *Applied Physics Letters* 86.8 (2005), pp. 1–3 (cit. on p. 37).

[40] V. P. Singh, B. Parsarathy, R. S. Singh, A. Aguilera, J. Anthony, and M. Payne. "Characterization of high-photovoltage CuPc-based solar

cell structures." In: *Solar Energy Materials and Solar Cells* 90.6 SPEC. ISS. (2006), pp. 798–812 (cit. on p. 37).

[41] SolarPower Europe. *Global Market Outlook for Solar Power 2015-2019*. Tech. rep. 2014, p. 32 (cit. on p. 2).

[42] Yanming Sun, Christopher J. Takacs, Sarah R. Cowan, Jung Hwa Seo, Xiong Gong, Anshuman Roy, and Alan J. Heeger. "Efficient, air-stable bulk heterojunction polymer solar cells using MoO x as the anode interfacial layer." In: *Advanced Materials* 23.19 (2011), pp. 2226–2230 (cit. on pp. 9, 27).

[43] Lew Tschugaeff. "Über das Thujen, ein neues bicyclisches Terpen." In: *Berichte der deutschen chemischen Gesellschaft* 33.3 (1900), p. 3118. URL: http://doi.wiley.com/10.1002/cber.19000330363 (cit. on p. 18).

[44] Paul A. VanHal, Martijn M. Wienk, Jan M. Kroon, Wiljan J. H. Verhees, Lenneke H. Slooff, Wouter J. H. VanGennip, Pascal Jonkheijm, and René A. J. Janssen. "Photoinduced electron transfer and photovoltaic response of a MDMO-PPV:TiO2 bulk-heterojunction." In: *Advanced Materials* 15.2 (2003), pp. 118–121. URL: http://doi.wiley.com/10.1002/adma.200390022 (cit. on pp. 9, 15).

[45] Matthew Wright and Ashraf Uddin. "Organic-inorganic hybrid solar cells: A comparative review." In: *Solar Energy Materials and Solar Cells* 107.July (2012), pp. 87–111 (cit. on p. 7).

[46] Zhengguo Xiao, Qingfeng Dong, Qi Wang, Wenjing Tian, Hui Huang, and Jinsong Huang. "Efficiency Enhancement in Polymer Solar Cells with a Polar Small Molecule Both at Interface and in the Bulk Heterojunction Layer." In: *IEEE Journal of Photovoltaics* (2015) (cit. on p. 9).

[47] K. Yoshino, K. Nomoto, A. Kinoshita, T. Ikari, Y. Akaki, and T. Yoshitake. "Dependence of Cu/In ratio of structural and electrical characterization of CuInS2 crystal." In: *Journal of Materials Science:*

Materials in Electronics 19.4 (2008), pp. 301–304. URL: http://link.springer.com/10.1007/s10854-007-9334-1 (cit. on p. 23).

[48] Guobing Zhang, Jie Zhang, Guanqun Ding, Jinghua Guo, Hongbo Lu, Longzhen Qiu, and Wanli Ma. "Synthesis and photovoltaic application of low-bandgap conjugated polymers by incorporating highly electron-deficient pyrrolo[3,4-d]pyridazine-5,7-dione units." In: *Polymer (United Kingdom)* 93 (2016), pp. 213–220. URL: http://dx.doi.org/10.1016/j.polymer.2016.04.011 (cit. on pp. 47, 48).

[49] Renjia Zhou and Jiangeng Xue. "Hybrid polymer-nanocrystal materials for photovoltaic applications." In: *ChemPhysChem* 13.10 (2012), pp. 2471–2480. URL: http://doi.wiley.com/10.1002/cphc.201101016 (cit. on p. 40).

[50] Renjia Zhou, Romain Stalder, Dongping Xie, Weiran Cao, Ying Zheng, Yixing Yang, Marc Plaisant, Paul H. Holloway, Kirk S. Schanze, John R. Reynolds, and Jiangeng Xue. "Enhancing the Efficiency of Solution-Processed Polymer: Colloidal Nanocrystal Hybrid Photovoltaic Cells Using Ethanedithiol Treatment." In: *ACS Nano* 7.6 (2013), pp. 4846–4854 (cit. on p. 40).

COLOPHON

This document was typeset using the typographical look-and-feel `classicthesis` developed by André Miede. The style was inspired by Robert Bringhurst's seminal book on typography "*The Elements of Typographic Style*". `classicthesis` is available for both LaTeX and LyX:

http://code.google.com/p/classicthesis/

Final Version as of August 24, 2016 (`classicthesis` version 4.2).